

Article

Neutral porphyrin derivative exerts anticancer activity by targeting cellular topoisomerase I (Top1) and promotes apoptotic cell death without stabilizing Top1-DNA cleavage complexes

Subhendu Kumar Das, Arijit Ghosh, Srijita Paul Chowdhuri, Nyancy Halder, Ishita Rehman, Souvik Sengupta, Krushna Chandra Sahoo, Harapriya Rath, and BENU BRATA DAS

J. Med. Chem., **Just Accepted Manuscript** • DOI: 10.1021/acs.jmedchem.7b01297 • Publication Date (Web): 30 Dec 2017

Downloaded from <http://pubs.acs.org> on December 30, 2017

Just Accepted

"Just Accepted" manuscripts have been peer-reviewed and accepted for publication. They are posted online prior to technical editing, formatting for publication and author proofing. The American Chemical Society provides "Just Accepted" as a free service to the research community to expedite the dissemination of scientific material as soon as possible after acceptance. "Just Accepted" manuscripts appear in full in PDF format accompanied by an HTML abstract. "Just Accepted" manuscripts have been fully peer reviewed, but should not be considered the official version of record. They are accessible to all readers and citable by the Digital Object Identifier (DOI®). "Just Accepted" is an optional service offered to authors. Therefore, the "Just Accepted" Web site may not include all articles that will be published in the journal. After a manuscript is technically edited and formatted, it will be removed from the "Just Accepted" Web site and published as an ASAP article. Note that technical editing may introduce minor changes to the manuscript text and/or graphics which could affect content, and all legal disclaimers and ethical guidelines that apply to the journal pertain. ACS cannot be held responsible for errors or consequences arising from the use of information contained in these "Just Accepted" manuscripts.



ACS Publications

Neutral porphyrin derivative exerts anticancer activity by targeting cellular topoisomerase I (Top1) and promotes apoptotic cell death without stabilizing Top1-DNA cleavage complexes

Subhendu Kumar Das ¹, Arijit Ghosh ¹, Srijita Paul Chowdhuri ¹, Nyancy Halder ², Ishita Rehman¹, Souvik Sengupta ^{1,3}, Krushna Chandra Sahoo ², Harapriya Rath, ^{2,*} and Benu Brata Das ^{1,*}

¹Laboratory of Molecular Biology, Department of Biological Chemistry; ²Department of Inorganic Chemistry; Indian Association for the Cultivation of Science, 2A & 2B, Raja S. C. Mullick Road, Jadavpur, Kolkata-700032, India. ³Division of Biological and Life Sciences, School of Arts and Sciences, Ahmedabad University, Central Campus, Navrangpura, Ahmedabad, Gujarat-380009, India.

*To whom correspondence should be addressed. Tel: +91 33 2473 4971 (Ext. 2108); Fax: +91 33 2473 2805; Email: pcbbd@iacs.res.in (BBD) and ichr@iacs.res.in (HR)

ABSTRACT

Camptothecin (CPT) selectively traps topoisomerase 1-DNA cleavable complexes (Top1cc) to promote anticancer activity. Here, we report the design, synthesis of a new class of neutral porphyrin derivative 5,10-bis(4-carboxyphenyl)-15, 20-bis(4-dimethylaminophenyl)-porphyrin (compound **8**), as a potent catalytic inhibitor of human Top1. In contrast to CPT, compound **8** reversibly binds with the free enzyme and inhibits the formation of Top1cc and promotes reversal of the preformed Top1cc with CPT. Compound **8** induced inhibition of Top1cc formation in live cells was substantiated by fluorescence recovery after photobleaching (FRAP) assays. We established that MCF7 cells treated with compound **8** triggers proteasome-mediated Top1 degradation, accumulates higher levels of reactive oxygen species (ROS), PARP1 cleavage, oxidative DNA fragmentation and stimulates apoptotic cell death without stabilizing apoptotic Top1-DNA cleavage complexes. Finally, compound **8** shows anticancer activity by targeting cellular Top1 and preventing the enzyme from directly participating in the apoptotic process.

Introduction

DNA topoisomerase I (Top1) are often exploited as imperative anticancer chemotherapeutic targets due to its critical role in DNA supercoil relaxation which involves three main steps: (a) DNA strand cleavage by a transesterification reaction initiated by the active site tyrosine attacking DNA phosphodiester backbone and generating a covalent intermediate of DNA 3'-phosphotyrosyl linkage (Top1cc), (b) DNA relaxation by controlled strand rotation and (c) DNA religation by a similar transesterification and release of the enzyme from the DNA.¹⁻⁵

Top1 inhibitors are classified into two groups, class I (poisons) and class II (catalytic inhibitors). Top1 poisons includes camptothecin (CPT), Topotecan, Irinotecan and other CPT derivatives as well as few non-CPT Top1 inhibitors like indenoisoquinolines, indolocarbazoles and thiohydantoin derivatives reveal their anticancer activity by selectively trapping the Top1-DNA covalent cleavage complexes (Top1cc) and inhibiting further religation of cleaved DNA strands.^{2, 3, 6, 7 8} Unrepaired Top1cc generates DNA double strand breaks following collision with replication or transcription machinery, which activate cell-cycle arrest and cell death.^{3, 9} In contrast, class II catalytic inhibitors hinder other steps of Top1 catalytic cycle by directly binding with enzyme but do not stabilize Top1cc which includes indolizinoquinolinedione.¹⁰⁻¹⁴ All types of topoisomerase inhibitors cause DNA breaks and are accountable for the killing of the proliferating cancer cells.^{3-5, 9}

Drug independent trapping of Top1cc's are also evidenced from endogenous DNA lesions, like UV and IR radiation-induced DNA damage, abasic sites, oxidized bases and mismatches.^{3, 9} Production of "apoptotic Top1cc" is independent of Top1 poisons but are dependent on variety of agents that are inducers of apoptotic cell death, including staurosporine, a protein kinase C inhibitor,¹⁵ Top2 inhibitor like etoposide and tubulin inhibitor like

1
2
3 vinblastine.¹⁶ All these compounds trigger cellular reactive oxygen species (ROS) that account
4
5 for oxidative DNA damages that promote stabilization of Top1cc.^{15, 17, 18}
6

7
8 Despite clinical success of CPT, the major limitations include its unstable chemical
9
10 structure, poor aqueous solubility, rapid cellular efflux *via* membrane pumps and acquisition of
11
12 cellular resistance of these drugs impelled the designing and investigation of new non-
13
14 camptothecin Top1 inhibitors.^{3, 4} Porphyrins are remarkably promising chemotype for
15
16 development of anticancer agents and photodynamic therapy, which includes FDA-approved and
17
18 clinically used sensitizer Photofrin.^{19, 20} Porphyrin derivatives have wide pharmaceutical
19
20 properties and broad range of biological activities that constitute selective modes of DNA
21
22 binding, mimicking photosynthetic centers, vitamin B12 and P-450,^{19, 21-24} nevertheless, the
23
24 cellular target of the compounds is still unclear.
25
26
27

28
29 Here, we discuss our study involving design, synthesis and biological evaluation of a
30
31 novel series of neutral porphyrin that inhibits human Top1. Selected neutral porphyrin derivative
32
33 5,10-bis(4-carboxyphenyl)-15,20-bis(4-dimethylaminophenyl)-porphyrin (compound **8**),
34
35 exhibited highest potency against human Top1 activity both as purified enzyme and as an
36
37 endogenous protein in the total cellular extracts of human breast adenocarcinoma (MCF7) cells
38
39 from our synthetic library. We have further established that the compound **8** binds with the free
40
41 enzyme and targets cellular Top1 for proteasome-mediated degradation and bolster ROS-induced
42
43 apoptotic cell death without stabilizing Top1-DNA cleavage complexes. Persistent with
44
45 inhibition of human Top1 activity *in vitro*, compound **8** was effective in killing cancer cells by
46
47 targeting cellular Top1.
48
49
50
51
52
53
54
55
56
57
58
59
60

Chemistry

The macrocycles under biological investigation described in our present manuscript are shown schematically (Scheme 1). We have taken into consideration, the parent basic porphyrin *i.e.* tetraphenyl porphyrin and variation in the periphery of the macrocycles with other *meso*-substituents. After investigating the biological properties of macrocycles compounds **1**, **2**, **3**, **4**, **5**, **6**, **7**, **9** and **10**, we designed and synthesized **8** following the literature known synthetic methodology. Synthesis of porphyrins, compounds **1**²⁵, **2**²⁶, **3**²⁷, **7**²⁸, **8**, **9** and **10**²⁹ were carried out following Adler Method,³⁰ macrocycles bearing four identical *meso*-substituents such as compound **1**, **2** and **10** were obtained by condensation of freshly distilled pyrrole and corresponding aryl aldehyde under reflux condition using propionic acid as an acidic solvent. Furthermore, synthesis of compound **3** and **8** (Scheme 1A) was tuned following the mixed-aldehyde condensation method leading to porphyrins bearing two different types of *meso*-substituents.³¹ The A₃B type of porphyrin, **7** and **9** are often obtained in mixed-aldehyde condensation methods and their yield was increased by reaction of 3:1 ratio of aldehydes A and B. It is a well-known fact that haloporphyrins undergo palladium-catalyzed cross-coupling reactions to produce alkyl-, vinyl-, aryl-, pyridyl- and alkynyl-porphyrin monomers, dimers, and oligomers.³² Thus, Suzuki-coupling was carried out by using strategically using mixture of **3** and 4-Aminophenylboronic acid pinacol ester to afford compound **4**³³ (Scheme 1A). Subsequently, the *trans*-substituted porphyrin, compound **5**³⁴ and **6** (Scheme 1B), were synthesized based on the MacDonald 2 + 2 condensation of dipyrromethane (synthesized by acid-catalyzed condensation of pyrrole with 4-bromobenzaldehyde) with 4-Pyridinecarboxaldehyde and 4-(pyridin-4-yl) benzaldehyde respectively.³⁵ Detailed spectroscopic characterization data,

1
2
3 elemental analysis and melting point of all the reported macrocycles in this manuscript have been
4
5 documented in the Experimental Section and the Supporting Information (S1 to S40).
6
7
8
9

10 **Biological Results and Discussion:**

11 12 13 14 **Neutral porphyrin derivative 8 inhibits human Topoisomerase 1 catalytic activity**

15
16
17 To test the inhibitory effect of the synthetic library of neutral porphyrin compounds
18
19 (Scheme 1) on human Top1 activity, we performed the DNA relaxation assays in a standard
20
21 assay mixture containing the plasmid DNA and recombinant Top1.^{6, 13, 36, 37} Table 1 enlists the
22
23 compounds with relative efficiencies of Top1 inhibition as a measure of their effective drug
24
25 concentrations (EC₅₀ value), indicating highest activity for the selected neutral porphyrin
26
27 derivative compound **8**.
28
29

30
31 To examine the mechanism of Top1 inhibition with compound **8** we used variable
32
33 incubation conditions in the relaxation assays (Figure 1A). When Top1 and compound **8** were
34
35 mixed together simultaneous in the relaxation assays (Figure 1A, lanes 13-16), 35-40 % Top1
36
37 inhibition was achieved at 1 μ M of compound **8** (Figure 1A, lane 16). Next to test the impact of
38
39 compound **8** interaction with Top1 in the relaxation assays, we pre-incubated Top1 with
40
41 compound **8** at indicated concentrations (Figure 1A, lanes 5-8) separately before the addition of
42
43 DNA.^{6, 13, 36, 38} Under these conditions, 1 μ M of compound **8** was sufficient to induce 85-95%
44
45 inhibition (Figure 1A, lane 8). Figure 1, panel A and D shows that Top1 inhibition was markedly
46
47 increased (~4-5 fold) when compound **8** was pre-incubated with the recombinant enzyme
48
49 compared to the simultaneous incubation (EC₅₀ for Top1 inhibition pre-incubation: 0.381 \pm 0.11
50
51
52
53
54
55
56
57
58
59
60

1
2
3 μM vs. simultaneous $1.472 \pm 0.32 \mu\text{M}$), suggesting that compound **8** may bind to the free
4
5 enzyme, unlike CPT to inhibit Top1 activity.
6

7
8 To investigate the selectivity of compound **8** towards endogenous Top1 in the whole cell
9
10 extracts of human breast adenocarcinoma (MCF7) cells (Figure 1B), we used *ex-vivo* Top1
11
12 relaxation inhibition assays.^{6, 39} The advantage of employing whole cell extracts as source of
13
14 Top1 is that the enzyme is maintained in its native structure among plethora of other proteins.
15
16 Figure 1C shows that compound **8** markedly inhibited Top1 activity when the cellular extracts
17
18 were pre-incubated with compound **8** (Figure 1C, lanes 5-10) compared to simultaneous
19
20 incubation (Figure 1, panel C, lanes 15-20). Quantification indicates that Top1 inhibition was
21
22 significantly increased (~2-3 fold) when compound **8** was pre-incubated with whole cell extracts
23
24 (Figure 1E), consistent with the inhibition of recombinant Top1 in pre-incubation relaxation
25
26 assays (Figure 1D).
27
28
29
30

31 Here we provide evidence that compound **8** selectively inhibit Top1, both as a purified
32
33 enzyme (Figure 1A) and as an endogenous protein in the total cellular lysate (Figure 1C) without
34
35 being afflicted by other proteins. Therefore, it is conceivable that compound **8** selectively
36
37 interacts with human Top1 to promote the inhibition of DNA relaxation activity.
38
39
40
41

42 **Compound 8 inhibits Top1-DNA cleavage complexes**

43
44 Because camptothecin (CPT) stabilizes Top1-DNA cleavable complexes (Top1cc) to
45
46 inhibit Top1 activity,^{3, 5, 37} we investigated compound **8** induced Top1cc formation with the
47
48 plasmid DNA cleavage assays.^{6, 8, 36, 37} Top1 mediated conversion of closed circular DNA (form
49
50 I) to nicked circular DNA (form II) in the presence of specific inhibitors are referred as
51
52 “cleavable complex”. Figure 2A shows that compound **8** failed to stabilize Top1cc in contrast to
53
54
55
56

CPT, suggesting that compound **8** inhibits Top1cc formation. To further investigate the impact of compound **8** on preformed Top1cc, we pre-incubated Top1 with plasmid DNA and CPT (Figure 2B) before the addition of compound **8** in the cleavage assays. Figure 2C shows that compound **8** completely abrogated CPT-induced Top1cc in a dose dependent manner (Figure 2, panel C, lanes 7-9).

In contrast to CPT (Figure 2D, lane 3), we further established that compound **8** failed to stabilize Top1cc in single turnover equilibrium cleavage assays (Figure 2D, lanes 4-6) by reacting recombinant Top1 with 25-mer duplex oligonucleotides harboring preferred Top1 cleavage sites.^{1, 13, 36, 38} In addition, compound **8** reversed the CPT-induced Top1cc with 12-mer cleaved oligonucleotides (Figure 2D, lane 7-9) consistent with plasmid DNA cleavage assays (Figure 2C). Taken together, our data indicate that compound **8** inhibits Top1 without trapping Top1cc.

To obtain direct evidence for compound **8** mediated inhibition of Top1cc formation in live human carcinoma cells, we used MCF7 cells and transiently expressed EGFP-Top1. Live cells expressing ectopic Top1 were analyzed under laser confocal microscopy equipped with fluorescence recovery after photobleaching (FRAP) technology⁴⁰⁻⁴². The FRAP recovery curves of EGFP-Top1 in the untreated samples represents a large (~80–85%) mobile population (see Figure 2E, and 2F; Ctr) compared to a small (~20%) immobile population, suggesting that Top1 is dynamic, freely exchanged and binds transiently with the DNA (reversible Top1cc).⁴²

However CPT covalently trapped Top1 on the DNA in the live cells (Figure 2E; CPT), which significantly impede FRAP recovery by increasing ~40–50% of Top1 immobile population (Figure 2E, and 2F; (+) CPT; 5 μ M). Under similar condition fluorescence recovery of EGFP-Top1 was unaffected in the presence of compound **8** (Figure 2E, and the quantification

in 2F; (+) compound **8**; 20 μ M), indicating compound **8** failed to trap Top1cc in live cells. Furthermore, compound **8** can restore ~12-15% of Top1 mobility in cells pretreated with CPT (Figure 2E-F), suggesting compound **8** promotes reversal of CPT-induced Top1cc in live cells consistent with the *in vitro* cleavage assays (Figure 2A-D). Taken together our data provide evidence that compound **8** inhibits cellular Top1cc formation.

Compound **8** reversibly binds with Top1 at equimolar concentration

Next we investigated the binding nature of compound **8** with the purified Top1 by measuring the intrinsic tryptophan fluorescence quenching of Top1. Figure 3A shows 1:1 binding stoichiometry of compound **8** with Top1 as measured from Job plot,^{12, 14, 43} suggesting that there is one binding site for the drug in the enzyme. Figure 3B and C shows the quenching profile of Top1 in the presence of variable doses of compound **8**, with a dissociation constant ($K_D = 0.381 \mu$ M) calculated from figure 3B and C.

To further investigate the nature of binding of compound **8** with Top1 (reversible vs. irreversible),^{12, 14} we performed dilution assay with recombinant Top1. Top1 was pre-incubated with 1 μ M of compound **8** at which 90–99% inhibition of enzyme has been achieved (Figure 3D, lane 4). The subsequent dilution of the reaction mixtures in the relaxation assays showed an increase in the % relief of inhibition for compound **8**. Complete relief of Top1 inhibition was achieved at 40-fold dilution (Figure 3D, lane 5-8). This suggests that compound **8** interact in reversible manner with Top1 consistent with its weak dissociation constant.

To investigate the intercalation capacity of the compound **8** into the plasmid DNA, we performed topoisomerase I unwinding assays^{36, 44}, which depends on the capacity of intercalating compounds to unwind the duplex DNA and thereby inducing a conformational

change in the DNA.^{36, 44} Figure 3E demonstrates that m-AMSA a strong DNA intercalative agent, incite a net negative supercoiling of the relaxed plasmid DNA at concentration independent manner (Figure 3E, lanes 3 and 4). Under similar conditions non-intercalative compounds like etoposide failed to show such effect (Figure 3E, lanes 5 and 6). Figure 3E, lanes 7, 8, 9 shows that compound **8** failed to induce negative supercoiling of the relaxed plasmid DNA at 50, 100, 300 μ M concentrations, suggesting neutral porphyrin derivative **8** is not a DNA intercalator. Therefore compound **8** interacts in reversible manner with Top1 to inhibit the plasmid relaxation activity (Figure 1).

Compound 8 triggers proteasome-mediated degradation of cellular Top1 without stabilizing apoptotic Top1-DNA covalent complexes

Because compound **8** binds with free Top1 (Figure 3) and inhibits Top1cc formation in live cells (Figure 2E), therefore we examined the impact of compound **8** on endogenous Top1. Cellular lysates were prepared from MCF7 cells treated with compound **8** for indicated times and were analyzed by Western blotting. Figure 4A, lanes 2-4 shows time dependent depletion of Top1 signal in compound **8** treated cells, suggesting Top1 degradation. Because proteasome has been implicated for Top1 degradation,^{7, 9, 45} thus we used proteasome specific inhibitor (MG132) to investigate Top1 proteolysis in compound **8** treated cells. Figure 4B confirmed that compound **8**-induced degradation of Top1 (Figure 4B, lane 2) was abrogated in the presence of proteasome inhibitor MG132 (Figure 4B, lane 4), suggesting compound **8** activates proteasome pathway.

Next, to investigate the plausibility between Top1 proteolysis and activation of apoptosis we tested PARP cleavage, a "hallmark" event of apoptosis in compound **8** treated cells.^{16-18, 46, 47}

Figure 4C shows compound **8** treatment for 12 h indeed promote PARP cleavage, suggesting compound **8** activates apoptosis through degradation of Top1.

Because compound **8** stimulates apoptosis (Figure 4C and Figure 5B), therefore we examined accumulation of apoptotic Top1-DNA complexes in compound **8** treated cells (Figure 4D) by ICE-bioassays.^{15, 16} Top1cc related to apoptosis are due to secondary DNA modifications and are independent from direct Top1-drug interaction.¹⁵⁻¹⁷ Under a condition that triggers PARP1 cleavage in MCF7 cells treated with compound **8**, immunoblotting revealed the absence of Top1 in the DNA-containing fractions (Figure 4D; compound **8**), in contrast to camptothecin (Figure 4D; CPT), indicating that compound **8** inhibits Top1cc during apoptosis. Compound **8** abrogates CPT-induced cellular Top1-DNA complexes (Figure 4D; CPT + **8**) in keeping with *in vitro* cleavage assays (Figure 2B). Therefore proteasome mediated degradation of Top1 triggers compound **8** induced apoptosis without stabilizing apoptotic Top1-DNA covalent complexes.

Compound **8 accumulates reactive oxygen species induced DNA breaks and promotes apoptotic cell death**

Next to investigate the mechanistic link between compound **8** induced cellular Top1 inhibition (Figure 1), degradation (Figure 4A and B) and activation of apoptosis (Figure 4C), we tested reactive oxygen species (ROS) formation and accumulation of oxidative DNA fragmentation^{15, 17, 46} in compound **8** treated MCF7 cells. To examine ROS accumulation, we used non fluorescent substrate (2',7'-dichlorodihydrofluorescein diacetate; H2DCFDA) which is transformed into fluorescent product (2',7'-dichlorofluorescein; DCF) in the presence of ROS inside the cells.¹³ Figure 5A shows time dependent accumulation of ROS in compound **8** treated cells. We observed a marked elevation (~3-5 fold) in ROS accumulation (Figure 5A) under

similar conditions that activate PARP1 cleavage (Figure 4C). Nonetheless, MCF7 cells pre-treated with N-acetyl-cysteine (NAC), a specific inhibitor of ROS, reduced compound **8** induced ROS generation by ~3-fold (Figure 5A).

One interpretation of this result is that compound **8** induced ROS may accumulate oxidative DNA strand breaks that activate apoptosis^{3, 13} as revealed by PARP1 cleavage (Figure 4C). Therefore, we directly measured compound **8** induced DNA strand breaks at single cellular level by using alkaline comet assays (Figure 5B-C), and simultaneously measured the apoptotic cell death by immunofluorescence staining of the apoptosis marker phosphatidylserine with Annexin V-FITC antibody (Figure 5D-E). Compound **8** treated MCF7 cells accumulate ~8-fold increase in DNA strand breaks (Figure 5B and C) compared to untreated cells resulting ~7-fold elevation in compound **8** induced Annexin V(+) apoptotic cells (Figure 5D and E). We further confirmed that ROS inhibitor NAC resulted ~4-fold decrease in compound **8** induced DNA breaks (Figure 5C) as well as ~4-5-fold reduction in Annexin V(+) apoptotic cells (Figure 5E). Therefore, we conclude compound **8** triggers reactive oxygen species induced DNA degradation and apoptotic cell death without stabilizing Top1-DNA cleavage complexes.

Compound **8** displays potent anticancer activity

Compound **8** was investigated for its cytotoxicity in the cancer cell lines from different tissue origin^{6, 41}, as well as in the non-cancerous human embryonic kidney cell lines (HEK293) and mouse embryonic fibroblasts (MEFs). Figure 6 indicates that compound **8** revealed potent cytotoxicity in cancerous cells including human breast adenocarcinoma cell lines (MCF7: IC₅₀: 2.17 μ M), human cervical cancer cell lines (HeLa: IC₅₀: 4.13 μ M), human ovarian adenocarcinoma cell lines (NIH:OVCAR-3: IC₅₀: 5.19 μ M) & human colon carcinoma cell lines

(HCT116: IC₅₀: 4.39 μ M) cells, compared to the non cancerous cells like HEK293 or MEFs that shows markedly reduced or no toxicity (IC₅₀: >10 μ M). The MCF7 breast cancer cell lines were most susceptible to compound **8**.

TDP1 hydrolyze 3' phosphotyrosyl linkages that are primarily due Top1cc, therefore TDP1^{-/-} cells are hypersensitive to Top1 poisons.^{40, 41, 45, 48} Figure 6F shows that both TDP^{-/-} and TDP1^{+/+} MEFs cells were equally sensitive to compound **8**, further providing evidence that compound **8** exerts cytotoxicity without stabilizing Top1cc (Figure 4D).

To further confirm that Top1 is the cellular target for compound **8** mediated cytotoxicity, we have performed cytotoxicity assays in siRNA mediated Top1 knockdown cells (Figure 6G, inset). Figure 6G indicate that compound **8** treated Top1 knockdown cells displayed reduced cytotoxicity compared to the Top1 proficient cells, establishing Top1 is the cellular target for compound **8**.

Because compound **8** exerts cytotoxicity without stabilizing Top1cc (Figure 4D), next we tested the impact of compound **8** on CPT-induced preformed Top1cc. Figure 6H shows that pretreatment of CPT and further addition of compound **8** were not additive in cytotoxicity, rather showed overlapping cytotoxicity in MCF7 cells treated with compound **8** or CPT independently. Therefore we conclude compound **8** plausibly suppress the CPT induced cytotoxicity (Figure 6H) because compound **8** reverse CPT-induced Top1cc formation in cells as well as in cleavage assays (Figure 2). Taken together these data suggest that compound **8** is a potential Top1 inhibitor and may be an appropriate lead to develop as a potential anticancer agent.

Conclusion

In summary, we have identified neutral porphyrin based compound **8** as a new potent anticancer agent which inhibits cellular Top1 without trapping Top1-DNA cleavage complexes, a mechanism which is unique in comparison to known Top1 poisons like camptothecin (CPT). We provide evidence that in contrast to CPT, the selected porphyrin derivative **8** binds reversibly to the free enzyme (Figure 3) and effectively inhibits the formation of Top1-DNA cleavage complex (Top1cc) both *in vitro* and in live cell as determined in FRAP assays (Figure 2). Compound **8** abrogates CPT-mediated preformed Top1cc both as recombinant enzyme (Figure 2A-D) and as an endogenous Top1 in the human breast adenocarcinoma (MCF7) cells (Figure 4D), suggesting a plausibility to overcome the limitations of CPT-resistance.

ROS-induced DNA damage facilitate trapping of Top1cc in cells is an obligatory event in the progression of apoptosis¹⁵⁻¹⁷. In contrast, compound **8** activates reactive oxygen species (ROS), proteolysis of cellular Top1, which may accumulate DNA torsional strain resulting oxidative DNA damage as revealed by alkaline comet assays and apoptotic cell death (Figure 5) without stabilization of apoptotic Top1-DNA complexes (Figure 4D). Therefore compound **8** counteracts the cellular Top1 by abrogating its precise engagement in the apoptotic process.

We further show that in contrast to non-cancerous cells, compound **8** is effective against cancerous cell lines from different tissue origin including MCF-7, HeLa, NIH:OVCA-3 and HCT116 cells (Figure 6) by targeting cellular Top1 (Figure 6G). Future challenge includes development of more potent neutral porphyrin based Top1 catalytic inhibitor, which may be exploited for anticancer therapy.

Experimental Section

Chemistry.

General Methods: Electronic absorption spectra were measured with a PerkinElmer Lambda 950 UV-visible-NIR spectrophotometer. ^1H NMR spectra were recorded on a Bruker AVIII 500 MHz spectrometer and chemical shifts were reported as the delta scale in ppm relative to CHCl_3 ($\delta = 7.26$ ppm) and DMSO ($\delta = 2.50$ ppm) as internal reference for ^1H . MALDI-TOF MS data were recorded using Bruker Daltonics flex Analyser. All solvents and chemicals were of reagent grade quality, obtained commercially and used without further purification except as noted. For spectral measurements, anhydrous dichloromethane was obtained by refluxing and distillation over CaH_2 . Gravity column chromatography was performed using Merck Silica Gel 230-400 mesh. All reported yields refer to pure isolated compounds. Chemicals and solvents were of reagent grade and used as obtained from commercial sources without further purification. The purities of all of the biologically tested compounds were the peak area of the major product was $\geq 95\%$ as estimated by NMR spectroscopy and C, H, N analysis along with melting point.

Synthesis:

5, 10, 15, 20-tetraphenylporphyrin (1): By using general method 1 mL (10 mmol) of benzaldehyde and 50 mL of propionic acid were mixed and the reaction mixture was magnetically stirred. Freshly distilled pyrrole (0.7 mL; 10 mmol) was then added to the mixture, the temperature then brought to reflux and allowed to stir for 2 hrs at reflux. After allowing the reaction mixture to cool to room temperature, the reaction flask was placed in the freezer overnight to aid precipitation of the porphyrin. The reaction mixture was then vacuum filtered using a sintered funnel and a dark purple solid was collected, washed with 5 x 50 mL of DCM,

washed with methanol and dried overnight and purified by silica gel chromatography to give 4.9g, of. 5,10,15,20-tetraphenylporphyrin (79% yields). mp> 300°C

¹H NMR (500 MHz, CDCl₃ 298 K, δ [ppm]): 8.88 (s, 8H, py), 8.25 (m, 8H, Ph-CH), 7.79 (m, 12H, Ph-CH), -2.76(s, 2H,-NH). **UV-VIS (CH₂Cl₂, λ [nm], 298 K):** 417nm, 515nm, 548nm, 590nm, 645 nm. **MALDI-TOF MS (m/z):** 615.635 (Calc. for C₄₄H₃₀N₄, exact mass: 614.206). **Elemental analysis:** Calcd for C₄₄H₃₀N₄ C, 85.97; H, 4.92; N, 9.11. Found: C, 86; H, 5.00; N, 9.08.

5, 10, 15, 20-tetrakis(4-carboxyphenyl)porphyrin (2): By using general method 1.5 g (10 mmol) of 4-formylbenzoic acid and 50 mL of propionic acid were added and the reaction mixture was stirred at ambient temperature. To increase the solubility of 4-formylbenzoic acid, the reaction mixture was heated to 80 °C at which point the aldehyde fully dissolved. Freshly distilled pyrrole (0.7 ml; 10 mmol) was then added to the mixture, and reaction mixture was allowed to stir for 2 hrs under reflux. The reaction mixture was cooled to room temperature, placed in the freezer overnight to aid precipitation of the porphyrin. The reaction mixture was then vacuum filtered using a sintered funnel and a dark purple solid was collected, washed with 5x50 mL of DCM, washed with methanol and dried overnight to give 1.1g, of. 5,10,15,20-tetrakis (4-carboxyphenyl) porphyrin (55% yields). mp> 300°C

¹H NMR (500 MHz, DMSO-d₆ 298 K, δ [ppm]): 13.14 (4H, br, -COOH), 8.86 (8H, s, Py β-H), 8.38 (16H, dd, phenyl H), -2.93 (2H, s, NH). **UV-VIS (CH₃OH, λ [nm], 298 K):** 413nm, 513nm, 545nm, 589nm, 646 nm. **MALDI-TOF MS (m/z):** 790.604 (Calc. for C₄₈H₃₀N₄O₈

exact mass: 790.206). **Elemental analysis:** Calcd for $C_{48}H_{30}N_4O_8$: C, 72.90; H, 3.82.; N, 7.09. Found: C, 73.00; H, 3.86; N, 7.07.

5,10-bis(4-bromophenyl)-15,20-di(4-pyridyl)porphyrin (3): By using general method 4-Pyridinecarboxaldehyde (0.535g, 5mmol), 4-bromobenzaldehyde (0.925g, 5 mmol) and 50 mL of propionic acid were added and the reaction mixture was stirred under nitrogen. To increase the solubility of 4-bromobenzaldehyde, the reaction mixture was heated to 80°C at which point the aldehyde fully dissolved. Freshly distilled pyrrole (0.7 mL; 10 mmol) was then added to the mixture, and allowed to stir for 4 hrs under reflux. Reaction mixture was brought to room temperature and the reaction flask was then placed in the freezer overnight to aid precipitation of the porphyrin. The crude product was repeatedly chromatographed on silica gel. The purest compound was obtained by recrystallization in methanol. Yield: 3.87g (50%). mp> 300°C

1H NMR (500 MHz, $CDCl_3$ 298 K, δ [ppm]): -2.86 (s, 2H, NH), 7.94 (d, J= 7.5Hz, 4H, Ph-Br), 8.10 (d, J= 7.5Hz, 4H, Ph-Br), 8.18 (d, J= 10 Hz, 4H, Pyridyl-H), 8.88 (m, 8H, β -H Py), 9.07 (d, J= 10 Hz, 4H, Pyridyl-H). **UV-VIS (CH_2Cl_2 , λ [nm], 298 K):** 418 nm, 514 nm, 547 nm, 588 nm, 645 nm. **MALDI-TOF MS (m/z):** 775.399 (Calc. for $C_{42}H_{26}Br_2N_6$ exact mass: 774.520). **Elemental analysis:** Calcd for $C_{42}H_{26}Br_2N_6$: C, 65.13; H, 3.38.; N, 10.85. Found: C, 65.14; H, 3.30; N, 10.72.

5,10-bis(4-aminobiphenyl)-15,20-bis(4-pyridyl)- porphyrin (4): A Schlenk tube was charged with 5,20-bis(4-bromophenyl)-10,15-di(pyridin-4-yl)porphyrin (0.054g, 0.07 mmol), 4-(4,4,5,5-

tetramethyl-1,3,2-dioxaborolan-2-yl)aniline (0.092g , 0.42 mmol) , K_3PO_4 (0.089g , 0.42 mmol) and $Pd(PPh_3)_4$ (8mg, 0.007mmol) under nitrogen atmosphere . Dioxane (5mL) and deionized water (0.1mL) were added and the resulting mixture was refluxed for 24 hours, brought to room temperature and filtered through celite in a sintered funnel. Washed several times with DCM, and the filtrate was evaporated in vacuum. The crude product obtained upon evaporation of solvent was purified by silica gel column chromatography (100-200 mesh) using ethyl acetate/dichloromethane (20:80, v/v) as an eluent. Yield 44.6 mg (80%). mp> 300°C

1H NMR (500 MHz, $CDCl_3$ 298 K, δ [ppm]): -2.76 (s, 2H, NH), 3.75 (s, 4H, NH_2), 6.88(d, 2H, J = 8.5Hz, β -H Py), 7.72 (d, 2H, J =8.5Hz, β -H Py), 7.91 (d, 4H, J =7.5Hz, Ph-H), 8.17 (d, 4H, J = 5.5Hz, Pyridyl-H), 8.20 (d, 4H, J = 8Hz, Ph-H), 8.81 (d, 4H, J = 4Hz, Ph-H), 8.84 (s, 2H, β -H Py), 8.97 (s, 2H, β -H Py), 9.01 (d, 4H, J = 4.5Hz, Ph-H), 9.03 (d, 4H, J = 5Hz, Pyridyl- H). **UV-VIS (CH_2Cl_2 , λ [nm], 298 K):** 420nm, 515 nm, 553nm, 592nm, 645 nm. **MALDI-TOF MS (m/z):** 798.820 (Calc. for $C_{54}H_{38}N_8$ exact mass: 798.322). **Elemental analysis:** Calcd for $C_{54}H_{38}N_8$: C, 81.18; H, 4.79.; N, 14.03. Found: C, 81.14; H, 4.16; N, 14.12.

5,15-bis(4-bromophenyl)-10,20-di(4-pyridyl)porphyrin (5): By using general method 2,2'-((4-bromophenyl)methylene)bis(1H-pyrrole) (0.5g, 1.66 mmol) and 4-pyridinecarboxaldehyde (0.171g, 1.6 mmol) were taken in a round bottom flask and 40 mL propionic acid was added to it. The reaction mixture was then stirred under nitrogen at 298K for 90 mins. Thereafter, the reaction mixture was refluxed under nitrogen for 90 minutes, brought to room temperature and left overnight for precipitation at room temperature. The precipitate was poured into sintered funnel and washed several times with methanol. The crude product thus obtained was vacuum

dried followed by repeated silica gel column chromatography. The purest compound was obtained by recrystallization from methanol. Yield 620mg (50%). mp> 300°C

¹H NMR (500 MHz, CDCl₃ 298 K, δ [ppm]): -2.85 (s, 2H, NH), 7.9 (d, J=8Hz, 4H, Ph-Br), 8.10 (d, J=7.5Hz, 4H, Ph-Br), 8.18 (d, J=5.5Hz, 4H, Pyridyl- H), 8.85 (br, 4H, β-H Py), 8.90 (br, 4H, β-H Py), 9.07 (d, J=5Hz, 4H, Pyridyl-H). **UV-VIS (CH₂Cl₂, λ [nm], 298 K):** 417nm, 513 nm, 548 nm, 590 nm, 644 nm. **MALDI-TOF MS (m/z):** 772.425 (Calc. for C₄₂H₂₆Br₂N₆ exact mass: 772.059). **Elemental analysis:** Calcd for for C₄₂H₂₆Br₂N₆: C, 65.13; H, 3.38.; N, 10.85. Found: C, 65.24; H, 3.40; N, 10.72.

5,15-bis(4-bromophenyl)-10,20-bis(4-phenylpyridyl)porphyrin (6): By using general method 2,2'-((4 bromophenyl)methylene)bis(1H-pyrrole) (0.5g, 1.66 mmol) and 4-(pyridin-4-yl)benzaldehyde (0.304g, 1.6 mmol) were taken in a round bottom flask and 40 mL propionic acid was added. The reaction mixture was then stirred under nitrogen at 298K for 90 mins. Thereafter, the reaction mixture was refluxed under nitrogen for 90 minutes, brought to room temperature and left overnight for precipitation. The precipitate was poured into sintered funnel and washed with methanol. The crude product left on the sintered funnel was then dried in vacuum. The crude product was purified by silica gel column chromatography (100-200 mesh) using ethyl acetate/dichloromethane (10:90, v/v) as an eluent. Yield: 296 mg (20%). mp> 300°C

¹H NMR (500 MHz, CDCl₃ 298 K, δ [ppm]): -2.81 (s, 2H, NH), 8.91 (br, 4H, Pyridyl-H), 8.87 (br, 2H, Py-βH), 8.85 (br, 4H, Pyridyl-H), 8.34 (d, J = 7.5Hz, 2H, Py-βH), 8.09 (m, 8H, 4-bromo Ph, Ph), 8.05 (d, J = 7.5 Hz, 2H, Py-βH), 7.92 (m, 8H, 4-bromo Ph, Ph), 7.86 (d, J= 5.5 Hz, 2H,

Py-βH), **UV-VIS (CH₂Cl₂, λ [nm], 298 K):** 418nm, 514 nm, 550 nm, 592 nm, 647 nm.

MALDI-TOF MS (m/z): 925.670 (Calc. for C₅₄H₃₄Br₂N₆ exact mass: 924.121). **Elemental**

analysis: Calcd for C₅₄H₃₄Br₂N₆: C, 69.99; H, 3.70.; N, 9.07. Found: C, 69.94; H, 3.64; N, 9.02.

5-(4-bromophenyl)-10,15,20-tri(4-pyridyl)porphyrin (7): By using general method 4-Pyridinecarboxaldehyde (1.605g, 15mmol), 4-bromobenzaldehyde (0.925g, 5 mmol) and 50 mL of propionic acid were added and the reaction mixture was magnetically stirred. Freshly distilled pyrrole (1.4 mL; 20 mmol) was then added to the mixture, the temperature then brought to reflux and allowed to stir for 4 hrs at reflux. After allowing the reaction mixture to cool to room temperature, the reaction flask was placed in the freezer overnight to aid precipitation of the porphyrin. The reaction mixture was then vacuum filtered using a sintered funnel and a dark purple solid was collected, washed with 5 x 50 mL of DCM, washed with methanol and dried overnight. The solid was purified by silica gel column chromatography. Yield 2.08 g (15%). mp> 300°C

¹H NMR (500 MHz, CDCl₃ 298 K, δ [ppm]): 9.06 (d, J= 5 Hz, 6H, Pyridyl-H), 8.90 (d, J= 4.5 Hz, 2H, β-H Py), 8.86 (s, 4H, β-H Py), 8.83 (d, J= 4.5 Hz, 2H, β-H Py), 8.17 (d, J= 5 Hz, 6H, Pyridyl-H), 8.07 (d, J= 8 Hz, 2H, Phenyl- H), 7.92 (d, J= 8 Hz, 2H, Phenyl- H). **UV-VIS (CH₂Cl₂, λ [nm], 298 K):** 416nm, 512nm, 547nm, 588nm, 643nm. **MALDI-TOF MS (m/z):** 696.658 (Calc. for C₄₁H₂₆BrN₇ exact mass: 696.612). **Elemental analysis:** Calcd for C₄₁H₂₆BrN₇: C, 70.69; H, 3.76.; N, 14.08. Found: C, 69.70; H, 3.86; N, 14.19.

5,10-bis(4-carboxyphenyl)-15,20-bis(4-dimethylaminophenyl)-porphyrin (8): By using general method 4(dimethylamino)benzaldehyde (0.745g, 5 mmol), 4-formylbenzoic acid (0.75g, 5mmol) and 50 mL of propionic acid were added and the reaction mixture was stirred under nitrogen. To increase the solubility of 4-formylbenzoic acid, the reaction mixture was heated to 80 °C at which point the aldehyde fully dissolved. Freshly distilled pyrrole (0.7 ml; 10 mmol) was then added to the reaction mixture and allowed to stir for 4 hrs under reflux. After allowing the reaction mixture to cool to room temperature, the reaction flask was placed in the freezer overnight to aid precipitation of the porphyrin. The precipitate was vacuum filtered through a sintered funnel and a dark purple solid so collected was washed with methanol and dried. The solid residue was purified over silica gel chromatography and recrystallized from methanol. Yield: 1.57g (20%). mp> 300°C

¹H NMR (500 MHz, DMSO-d₆ 298 K, δ [ppm]): 12.85 (2H, br, -COOH), 8.96 (br, 4H, CarboxyPh-CH), 8.82 (br, 6H, CarboxyPh-CH and Py-β-CH), 8.38 (d, J = 7.5 Hz, 4H, N,N-Dimethyl Ph), 8.33 (d, J = 7.5 Hz, 4H, N,N-Dimethyl Ph), 8.03 (d, J = 7.5 Hz, 2H, Py-β-CH), 7.95 (s, 2H, Py-β-CH), 7.16 (d, J = 8 Hz, 2H, Py-β-CH), 2.89 (s, 12H, Me), -2.84 (br, 2H, NH). **UV-VIS (CH₂Cl₂, λ [nm], 298 K):** 414 nm, 516 nm, 557 nm, 594 nm, 652 nm. **MALDI-TOF MS (m/z):** 788.681 (Calc. for C₅₀H₄₀N₆O₄ exact mass: 788.311). **Elemental analysis:** Calcd for C₅₀H₄₀N₆O₄: C, 76.12; H, 5.11.; N, 10.65. Found: C, 76.14; H, 5.16; N, 10.62.

5-(4-carboxyphenyl)-10,15,20-tri(4-dimethylaminophenyl)- porphyrin (9): By using general method 4(dimethylamino)benzaldehyde (2.23g, 15 mmol), 4-formylbenzoic acid (0.75g, 5mmol) were added to 50 mL of propionic acid and the reaction mixture was magnetically

1
2
3 stirred. Freshly distilled pyrrole (1.4 ml; 20 mmol) was then added to the mixture, the
4
5 temperature then brought to reflux and allowed to stir for 4 hrs at reflux. After allowing the
6
7 reaction mixture to cool to room temperature, the reaction flask was placed in the freezer
8
9 overnight to aid precipitation of the porphyrin. The reaction mixture was then vacuum filtered
10
11 using a sintered funnel and a dark purple solid was collected, washed with 5x50 mL of DCM,
12
13 washed with methanol and dried overnight. The solid residue was purified over silica gel
14
15 chromatography using 30% EtOAc-CH₂Cl₂. Yield 3.1g (20%). mp> 300°C
16
17
18

19
20 **¹H NMR (500 MHz, CDCl₃ 298 K, δ [ppm]):** 12.85 (1H, br, -COOH), 8.92 (br, 2H,
21
22 CarboxyPh-CH), 8.75 (br, 2H, CarboxyPh-CH), 8.57 (s, 4H, Py-β-CH), 8.42 (br, 6H, N,N-
23
24 Dimethyl Ph), 8.28 (br, 6H, N,N- Dimethyl Ph), 8.06 (d, J = 7 Hz, 2H, Py-β-CH), 7.10 (d, J = 7
25
26 Hz, 2H, Py-β-CH), 3.32 (s, 18H, Me), -2.70 (br, 2H, NH). **UV-VIS (CH₂Cl₂, λ [nm], 298 K):**
27
28 417 nm, 519 nm, 561 nm, 598nm, 655 nm. **MALDI-TOF MS (m/z):** 787.918 (Calc. for
29
30 C₅₁H₄₅N₇O₂ exact mass: 787.363). Elemental analysis: Calcd for C₅₁H₄₅N₇O₂:C, 77.74; H, 5.76.;
31
32 N, 12.44. Found: C, 77.80; H, 5.81; N, 12.41.
33
34
35
36
37
38
39
40

41 **5,10,15,20-tetra(4-pyridyl)porphyrin (10)** : By using general method 1.07 g (10 mmol) of 4-
42
43 Pyridinecarboxaldehyde and 50 mL of propionic acid were added and the reaction mixture was
44
45 magnetically stirred. Freshly distilled pyrrole (0.7 mL; 10 mmol) was then added to the mixture,
46
47 the temperature then brought to reflux and allowed to stir for 2 hrs at reflux. After allowing the
48
49 reaction mixture to cool to room temperature, the reaction flask was placed in the freezer
50
51 overnight to aid precipitation of the porphyrin. The reaction mixture was then vacuum filtered
52
53 using a sintered funnel and a dark purple solid was collected, washed with 5 x 50 mL of DCM,
54
55
56
57
58
59
60

washed with methanol and dried overnight to give 5,10,15,20-tetra(4-pyridyl)porphyrin .Yield 2.472 g (20%). mp> 300°C

¹H NMR (500 MHz, CDCl₃ 298 K, δ [ppm]): 8.94 (d, J= 5 Hz, 8H, Pyridyl-H), 8.79(b, 8H, Pyrrole β-H), 8.16 (d, J= 5 Hz, 8H, Pyridyl- H), -2.99 (b, 2H, pyrrole NH). **UV-VIS (CH₂Cl₂, λ [nm], 298 K):** 415nm, 511nm, 545nm, 587nm, 642nm. **MALDI-TOF MS (m/z):** 618.629 (Calc. for C₄₀H₂₆N₈ exact mass: 618.704). Elemental analysis: Calcd for C₄₀H₂₆N₈: C, 77.65; H, 4.24.; N, 18.11. Found: C, 77.00; H, 4.16; N, 18.07.

Drug and antibodies

Camptothecin, proteasomal inhibitor MG132 and N-acetyl-L-Cysteine (NAC) were purchased from Sigma. Mouse monoclonal anti-human Top1 (C21) antibody, rabbit polyclonal PARP1 antibody and secondary antibodies: horseradish peroxidase conjugated anti-rabbit IgG or anti-mouse IgG were obtained from Santa Cruz Biotechnology (USA). Anti-actin (ACTN05) antibody was from Neo Markers (USA).

Recombinant human topoisomerase 1 and plasmid DNA relaxation assay

The recombinant human Top1 was purified from Sf-9 insect cells, infected with the recombinant baculovirus (a kind gift from Prof. James. J. Champoux) as described previously.⁶

13

The types 1 DNA topoisomerase are assayed by decreased mobility of the relaxed isomers of supercoiled pBS (SK⁺) DNA in 1% agarose gel. The relaxation assay was carried out with recombinant human Top1 or the whole cell extracts of human breast adenocarcinoma

(MCF7) cells as source of endogenous Top1, diluted in the relaxation buffer with supercoiled plasmid DNA as described previously.^{6, 8, 13, 38}

Cleavage assay

Plasmid DNA cleavage assay was carried out as described previously^{6, 8}. Equilibrium Cleavage assays with 25-mer duplex of oligonucleotide containing a Top1 binding motif was labeled and annealed as described previously.^{13, 36, 38} Samples were analyzed by 12 % sequencing gel electrophoresis, dried and exposed on PhosphorImager screens and imaged with Typhoon FLA 7000 (GE Healthcare, UK).

Cell culture and transfection

Human cancerous cell lines like MCF7, HeLa, HCT116, NIH: OVCAR-3 and HEK293 were obtained from the Developmental Therapeutics Program as kind gift from Dr. Yves Pommier (NIH/NCI/USA), TDP1^{+/+} and TDP1^{-/-} primary MEF cells were kind gift from Dr Cornelius F Boerkoel (University of British Columbia, Canada) were cultured as described previously.^{6, 36, 40, 42} Plasmid DNAs were transfected with Lipofectamine 2000 (Invitrogen) according to the manufacturer's protocol.

Photobleaching experiments

Photobleaching experiments were performed as described formerly⁴⁰⁻⁴² using Andor Spinning disc inverted confocal laser-scanning microscope equipped with a 60X/1.42 NA oil-immersion objective (Olympus) and with a CO₂-controlled on-stage heated environmental chamber set to 37°C. FRAP analyses were carried out with living MCF7 cells ectopically

expressing EGFP-human Top1 grown on chamber cover glass (Genetix, India) and drug treated as indicated. For FRAP analysis, a subnuclear spot was bleached for 30 ms by solid-state laser line (488 nm for EGFP) adapted to the fluorescent protein of interest and FRAP curves were generated individually normalized to the pre-bleach signal as described previously.⁴²

Job plot and Spectrofluorimetric binding assay

The binding stoichiometry for compound **8** with Top1 was determined using the method of continuous variation^{12, 14, 43}. Briefly, reaction mixtures containing variable Top1 and compound **8** to a final concentration of 1.25 μ M were analyzed for quenching of tryptophan fluorescence at 350 nm upon excitation at 295 nm on PerkinElmer LS55 luminescence spectrometer.

Spectrofluorimetric binding assay was carried out as previously^{12, 14, 43} where Top1 (200 nM) was incubated with various concentrations of compound **8** (0 to 11 μ M) at 25⁰C for 10 min. The equation for determining fraction of binding sites (B) occupied by inhibitor was $B = (F_0 - F) / F_{\max}$, where F_0 is the fluorescence intensity at 350 nm of Top1 alone in the absence of any inhibitors, F is the fluorescence intensity at 350 nm of Top1 in the presence of inhibitor, and F_{\max} is obtained from the plot of $1/(F_0 - F)$ versus $1/[X]$ and by extrapolating $1/[X]$ to zero, where $[X]$ is the concentration of compound **8**. The dissociation constant (K_D) was determined as described previously.¹²

Analysis of compound **8**-DNA intercalation

The competence of the drug to intercalate into plasmid DNA was determined by Top1 unwinding assay.^{36, 44} Assays were performed with 50 fmol of pBluscript (SK+) DNA in the

1
2
3 presence or absence of compound 8, m-AMSA and etoposide at indicated concentrations. Excess
4
5 of DNA topoisomerase I was reacted with supercoiled plasmid DNA to generate relaxed DNA
6
7 for the unwinding assays. The relaxed DNA was purified by proteolytic digestion with proteinase
8
9 K at 37°C, followed by phenol / chloroform extraction and ethanol precipitation. The unwinding
10
11 assays were carried out at 37°C for 15 min with independent compounds, and were analyzed by
12
13 1% agarose gel as described above.
14
15
16
17
18

19 **Cell extracts and immunoblotting**

20
21 Preparation of whole cell extracts from MCF7 cells and immunoblotting were carried out
22
23 as described.^{6, 40, 41} Immunoreactivity was detected using ECL chemiluminescence reaction
24
25 (Amersham) under ChemiDocTM MP System (Bio-Rad, USA).
26
27
28
29
30

31 **Immuno Complex of Enzyme (ICE) Bioassay**

32
33 *In vivo* Top1 cleavage complexes (Top1cc) were isolated from MCF7 cells using immuno
34
35 complex of enzyme (ICE) bioassay technique.⁴⁹ Briefly, 5×10^6 MCF7 cells were treated with
36
37 drugs and were lysed by DNazol reagent (Invitrogen, USA) in the presence of 0.1% SDS.
38
39 Genomic DNA was prepared and was briefly sonicated. Varying concentrations of DNA were
40
41 spotted onto nitrocellulose membrane (Millipore, USA) using a slot-blot vacuum system (Bio-
42
43 rad, USA). Immunoblotting were carried out with anti-human Top1 antibodies as described.⁴¹
44
45
46
47
48

49 **Measurement of ROS**

50
51 Intracellular ROS was detected in drug-treated MCF7 cells with or without pretreatment
52
53 of N-acetyl-L-cysteine (NAC) for indicated time as described.^{13, 46} Briefly, cells were washed
54
55
56
57
58
59
60

and resuspended in 500 μ L of $1\times$ PBS and were loaded with 2 μ g/mL of H₂DCFDA (Molecular Probes) for 30 min, and green fluorescence of 2,7-dichlorofluorescein was measured at 515 nm by spectrofluorometer.

Alkaline COMET assays

To detect the levels of drug-induced DNA breaks, after treatment MCF7 cells were subjected to alkaline comet assays according to the manufacturer's instructions (Trevigen, USA), comet length was measured and was scored for at least 50 cells. Distributions of comet lengths were compared using the Student *t*-test as described previously.^{13, 40, 50}

Immunocytochemistry

Immunofluorescence staining of apoptosis marker phosphatidylserine was performed as described previously.^{40, 41} After treatment, MCF7 cells were fixed with 2% paraformaldehyde for 10 min at room temperature and stained with Annexin V-FITC antibody (BD, USA), mounted in anti-fade solution with propidium iodide (Vector Laboratories, USA) and examined under Leica TCS SP8 confocal laser-scanning microscope.

Cell survival assay

Cell survival was assessed by 3-(4,5-dimethylthiazol-2-yl)-2,5-diphenyltetrazolium bromide (MTT) assay as discussed previously.⁶ The percent inhibition of viability for each concentration of the compounds was calculated with respect to the control and IC₅₀ values were estimated.

siRNA transfection

Transfections were performed as described previously.⁴⁰ In brief, cells (1.5×10^5) were transfected with control siRNA or 40 nM Top1 siRNA (Qiagen) using oligofectamine (Invitrogen) according to the manufacturer's protocol. Time course experiments revealed a maximum suppression of Top1 protein at day 3 after transfection, as analyzed by Western blotting.

Supporting Information:

The supporting information is available free of charge on the ACS website

MALDI-TOF MS, ^1H NMR, ^1H - ^1H 2D COSY Spectra, and UV-VIS data of compounds 1 to 10 are provided in the Supporting information (PDF).

Molecular String Formula and some data (CSV)

Acknowledgment

We wish to thank Dr. Hemanta K Majumder and Dr. Suvendra N Bhattacharyya, CSIR-Indian Institute of Chemical Biology, India for the help during the study. The BBD team is supported by Wellcome Trust / DBT India Alliance Intermediate Fellowship (Award# IA/I/13/1/500888). AG and KCS are recipients of CSIR-NET-Senior Research Fellowship, India. SPC thank to UGC-CSIR-NET for Junior Research Fellowship. SKD, IR and NH thank IACS for SRF and JRF positions respectively. HR thank DST-SERB (EMR/2016/004705) for the research grant. BBD is a Wellcome Trust / DBT India Alliance Intermediate fellow.

CONFLICT OF INTEREST

None declared.

REFERENCES

1. Champoux, J. J. DNA topoisomerases: structure, function, and mechanism. *Annu Rev Biochem* **2001**, *70*, 369-413.
2. Capranico, G.; Marinello, J.; Chillemi, G. Type I DNA topoisomerases. *J. Med. Chem* **2017**, *60*, 2169-2192.
3. Pommier, Y. Drugging topoisomerases: lessons and challenges. *ACS Chemical Biology* **2013**, *8*, 82-95.
4. Pommier, Y. DNA topoisomerase I inhibitors: chemistry, biology, and interfacial inhibition. *Chem Rev* **2009**, *109*, 2894-2902.
5. Pommier, Y. Topoisomerase I inhibitors: camptothecins and beyond. *Nat Rev Cancer* **2006**, *6*, 789-802.
6. Majumdar, P.; Bathula, C.; Basu, S. M.; Das, S. K.; Agarwal, R.; Hati, S.; Singh, A.; Sen, S.; Das, B. B. Design, synthesis and evaluation of thiohydantoin derivatives as potent topoisomerase I (top1) inhibitors with anticancer activity. *Eur J Med Chem* **2015**, *102*, 540-551.
7. Nagarajan, M.; Morrell, A.; Antony, S.; Kohlhagen, G.; Agama, K.; Pommier, Y.; Ragazzon, P. A.; Garbett, N. C.; Chaires, J. B.; Hollingshead, M.; Cushman, M. Synthesis and biological evaluation of bisindenoisoquinolines as topoisomerase I inhibitors. *J. Med. Chem* **2006**, *49*, 5129-5140.
8. Cushman, M.; Jayaraman, M.; Vroman, J. A.; Fukunaga, A. K.; Fox, B. M.; Kohlhagen, G.; Strumberg, D.; Pommier, Y. Synthesis of new indeno[1,2-c]isoquinolines: cytotoxic non-camptothecin topoisomerase I inhibitors. *J. Med. Chem* **2000**, *43*, 3688-3698.
9. Pommier, Y.; Sun, Y.; Huang, S. N.; Nitiss, J. L. Roles of eukaryotic topoisomerases in transcription, replication and genomic stability. *Nat Rev Mol Cell Biol* **2016**, *17*, 703-721.
10. Wu, N.; Wu, X. W.; Agama, K.; Pommier, Y.; Du, J.; Li, D.; Gu, L. Q.; Huang, Z. S.; An, L. K. A novel DNA topoisomerase I inhibitor with different mechanism from camptothecin induces G2/M phase cell cycle arrest to K562 cells. *Biochemistry* **2010**, *49*, 10131-10136.
11. Yu, L. M.; Zhang, X. R.; Li, X. B.; Yang, Y.; Wei, H. Y.; He, X. X.; Gu, L. Q.; Huang, Z. S.; Pommier, Y.; An, L. K. Synthesis and biological evaluation of 6-substituted indolizinoquinolinediones as catalytic DNA topoisomerase I inhibitors. *Eur J Med Chem* **2015**, *101*, 525-533.
12. Chowdhury, S.; Mukherjee, T.; Sengupta, S.; Chowdhury, S. R.; Mukhopadhyay, S.; Majumder, H. K. Novel betulin derivatives as antileishmanial agents with mode of action targeting type IB DNA topoisomerase. *Mol Pharmacol* **2011**, *80*, 694-703.

13. Ganguly, A.; Das, B.; Roy, A.; Sen, N.; Dasgupta, S. B.; Mukhopadhyay, S.; Majumder, H. K. Betulinic acid, a catalytic inhibitor of topoisomerase I, inhibits reactive oxygen species-mediated apoptotic topoisomerase I-DNA cleavable complex formation in prostate cancer cells but does not affect the process of cell death. *Cancer Res* **2007**, *67*, 11848-11858.
14. Saha, S.; Acharya, C.; Pal, U.; Chowdhury, S. R.; Sarkar, K.; Maiti, N. C.; Jaisankar, P.; Majumder, H. K. A novel spirooxindole derivative inhibits the growth of *Leishmania donovani* parasites both in vitro and in vivo by targeting type IB topoisomerase. *Antimicrob Agents Chemother* **2016**, *60*, 6281-6293.
15. Sordet, O.; Khan, Q. A.; Plo, I.; Pourquier, P.; Urasaki, Y.; Yoshida, A.; Antony, S.; Kohlhagen, G.; Solary, E.; Saparbaev, M.; Laval, J.; Pommier, Y. Apoptotic topoisomerase I-DNA complexes induced by staurosporine-mediated oxygen radicals. *J Biol Chem* **2004**, *279*, 50499-50504.
16. Sordet, O.; Goldman, A.; Pommier, Y. Topoisomerase II and tubulin inhibitors both induce the formation of apoptotic topoisomerase I cleavage complexes. *Mol Cancer Ther* **2006**, *5*, 3139-3144.
17. Sen, N.; Banerjee, B.; Das, B. B.; Ganguly, A.; Sen, T.; Pramanik, S.; Mukhopadhyay, S.; Majumder, H. K. Apoptosis is induced in leishmanial cells by a novel protein kinase inhibitor withaferin A and is facilitated by apoptotic topoisomerase I-DNA complex. *Cell Death Differ* **2007**, *14*, 358-367.
18. Sordet, O.; Goldman, A.; Redon, C.; Solier, S.; Rao, V. A.; Pommier, Y. Topoisomerase I requirement for death receptor-induced apoptotic nuclear fission. *Journal of Biological Chemistry* **2008**, *283*, 23200-23208.
19. Teo, R. D.; Hwang, J. Y.; Termini, J.; Gross, Z.; Gray, H. B. Fighting cancer with corroles. *Chemical Reviews* **2017**, *117*, 2711-2729.
20. Zou, Q.; Abbas, M.; Zhao, L.; Li, S.; Shen, G.; Yan, X. Biological photothermal nanodots based on self-assembly of peptide-porphyrin conjugates for antitumor therapy. *Journal of the American Chemical Society* **2017**, *139*, 1921-1927.
21. Karunakaran, S. C.; Ramaiah, D.; Schulz, I.; Epe, B. Study of the mode and efficiency of DNA binding in the damage induced by photoactivated water soluble porphyrins. *Photochem Photobiol* **2013**, *89*, 1100-1105.
22. Munson, B. R.; Fiel, R. J. DNA intercalation and photosensitization by cationic meso substituted porphyrins. *Nucleic Acids Research* **1992**, *20*, 1315-1319.
23. Shuai, L.; Wang, S.; Zhang, L.; Fu, B.; Zhou, X. Cationic porphyrins and analogues as new DNA topoisomerase I and II inhibitors. *Chem Biodivers* **2009**, *6*, 827-837.

24. Zhai, B.; Shuai, L.; Yang, L.; Weng, X.; Wu, L.; Wang, S.; Tian, T.; Wu, X.; Zhou, X.; Zheng, C. Octa-substituted anionic porphyrins: topoisomerase I inhibition and tumor cell apoptosis induction. *Bioconjug Chem* **2008**, *19*, 1535-1542.
25. Adler, A. D.; Longo, F. R.; Finarelli, J. D.; Goldmacher, J.; Assour, J.; Korsakoff, L. A simplified synthesis for meso-tetraphenylporphine. *The Journal of Organic Chemistry* **1967**, *32*, 476-476.
26. Harada, A.; Yamaguchi, H.; Okamoto, K.; Fukushima, H.; Shiotsuki, K.; Kamachi, M. Control of photoinduced electron transfer from zinc-porphyrin to methyl viologen by supramolecular formation between monoclonal antibody and zinc-porphyrin. *Photochem Photobiol* **1999**, *70*, 298-302.
27. Fouad, F. S.; Crasto, C. F.; Lin, Y.; Jones, G. B. Photoactivated enediynes: targeted chimeras which undergo photo-bergman cyclization. *Tetrahedron Letters* **2004**, *45*, 7753-7756.
28. Ikeda, T.; Shinkai, S.; Sada, K.; Takeuchi, M. A preliminary step toward molecular spring driven by cooperative guest binding. *Tetrahedron Letters* **2009**, *50*, 2006-2009.
29. Smith, M. W.; Lawton, L. G.; Checkoff, J. Tetrapyrrolyl porphyrin derivatives of group 13 metals. *Synthesis and Reactivity in Inorganic and Metal-Organic Chemistry* **1993**, *23*, 639-651.
30. Adler, A. D.; Sklar, L.; Longo, F. R.; Finarelli, J. D.; Finarelli, M. G. A mechanistic study of the synthesis of meso-tetraphenylporphyrin. *Journal of Heterocyclic Chemistry* **1968**, *5*, 669-678.
31. Zhang, X.-X.; Wayland, B. B. Rhodium(II) porphyrin bimetallo-radical complexes: preparation and enhanced reactivity with CH₄ and H₂. *Journal of the American Chemical Society* **1994**, *116*, 7897-7898.
32. DiMaggio, S. G.; Lin, V. S. Y.; Therien, M. J. Catalytic conversion of simple haloporphyrins into alkyl-, aryl-, pyridyl-, and vinyl-substituted porphyrins. *Journal of the American Chemical Society* **1993**, *115*, 2513-2515.
33. Hyslop, A. G.; Therien, M. J. Synthesis of porphyrin-spacer-quinone compounds via metal-mediated cross-coupling: new systems for probing the relative magnitudes of axial and equatorial electronic coupling at the porphyrin macrocycle in thermal and photoactivated electron transfer reactions. *Inorganica Chimica Acta* **1998**, *275*, 427-434.
34. Nowak-Król, A.; Koszarna, B.; Yoo, S. Y.; Chromiński, J.; Węclawski, M. K.; Lee, C.-H.; Gryko, D. T. Synthesis of trans-A₂B₂-porphyrins bearing phenylethynyl substituents. *The Journal of Organic Chemistry* **2011**, *76*, 2627-2634.

35. Ravikanth, M.; Strachan, J.-P.; Li, F.; Lindsey, J. S. Trans-substituted porphyrin building blocks bearing iodo and ethynyl groups for applications in bioorganic and materials chemistry. *Tetrahedron* **1998**, *54*, 7721-7734.
36. Das, B. B.; Sen, N.; Roy, A.; Dasgupta, S. B.; Ganguly, A.; Mohanta, B. C.; Dinda, B.; Majumder, H. K. Differential induction of *Leishmania donovani* bi-subunit topoisomerase I-DNA cleavage complex by selected flavones and camptothecin: activity of flavones against camptothecin-resistant topoisomerase I. *Nucleic Acids Res* **2006**, *34*, 1121-1132.
37. Gentry, A. C.; Juul, S.; Veigaard, C.; Knudsen, B. R.; Osheroff, N. The geometry of DNA supercoils modulates the DNA cleavage activity of human topoisomerase I. *Nucleic Acids Res* **2011**, *39*, 1014-1022.
38. Das, B. B.; Sen, N.; Dasgupta, S. B.; Ganguly, A.; Majumder, H. K. N-terminal region of the large subunit of *Leishmania donovani* bisubunit topoisomerase I is involved in DNA relaxation and interaction with the smaller subunit. *Journal of Biological Chemistry* **2005**, *280*, 16335-16344.
39. Marchand, C.; Huang, S. Y.; Dexheimer, T. S.; Lea, W. A.; Mott, B. T.; Chergui, A.; Naumova, A.; Stephen, A. G.; Rosenthal, A. S.; Rai, G.; Murai, J.; Gao, R.; Maloney, D. J.; Jadhav, A.; Jorgensen, W. L.; Simeonov, A.; Pommier, Y. Biochemical assays for the discovery of TDP1 inhibitors. *Mol Cancer Ther* **2014**, *13*, 2116-2126.
40. Das, B. B.; Antony, S.; Gupta, S.; Dexheimer, T. S.; Redon, C. E.; Garfield, S.; Shiloh, Y.; Pommier, Y. Optimal function of the DNA repair enzyme TDP1 requires its phosphorylation by ATM and/or DNA-PK. *Embo j* **2009**, *28*, 3667-3680.
41. Das, B. B.; Huang, S. Y.; Murai, J.; Rehman, I.; Ame, J. C.; Sengupta, S.; Das, S. K.; Majumdar, P.; Zhang, H.; Biard, D.; Majumder, H. K.; Schreiber, V.; Pommier, Y. PARP1-TDP1 coupling for the repair of topoisomerase I-induced DNA damage. *Nucleic Acids Res* **2014**, *42*, 4435-4449.
42. Das, S. K.; Rehman, I.; Ghosh, A.; Sengupta, S.; Majumdar, P.; Jana, B.; Das, B. B. Poly(ADP-ribose) polymers regulate DNA topoisomerase I (Top1) nuclear dynamics and camptothecin sensitivity in living cells. *Nucleic Acids Res* **2016**, *44*, 8363-8375.
43. Huang, C. Y. Determination of binding stoichiometry by the continuous variation method: the Job plot. *Methods Enzymol* **1982**, *87*, 509-525.
44. Chen, G. L.; Yang, L.; Rowe, T. C.; Halligan, B. D.; Tewey, K. M.; Liu, L. F. Nonintercalative antitumor drugs interfere with the breakage-reunion reaction of mammalian DNA topoisomerase II. *J Biol Chem* **1984**, *259*, 13560-13566.
45. Pommier, Y.; Huang, S. Y.; Gao, R.; Das, B. B.; Murai, J.; Marchand, C. Tyrosyl-DNA-phosphodiesterases (TDP1 and TDP2). *DNA Repair (Amst)* **2014**, *19*, 114-129.

46. Sen, N.; Das, B. B.; Ganguly, A.; Mukherjee, T.; Tripathi, G.; Bandyopadhyay, S.; Rakshit, S.; Sen, T.; Majumder, H. K. Camptothecin induced mitochondrial dysfunction leading to programmed cell death in unicellular hemoflagellate *Leishmania donovani*. *Cell Death Differ* **2004**, *11*, 924-936.
47. Soldani, C.; Scovassi, A. I. Poly(ADP-ribose) polymerase-1 cleavage during apoptosis: an update. *Apoptosis* **2002**, *7*, 321-328.
48. Hirano, R.; Interthal, H.; Huang, C.; Nakamura, T.; Deguchi, K.; Choi, K.; Bhattacharjee, M. B.; Arimura, K.; Umehara, F.; Izumo, S.; Northrop, J. L.; Salih, M. A.; Inoue, K.; Armstrong, D. L.; Champoux, J. J.; Takashima, H.; Boerkoel, C. F. Spinocerebellar ataxia with axonal neuropathy: consequence of a TDP1 recessive neomorphic mutation? *Embo j* **2007**, *26*, 4732-4743.
49. Regairaz, M.; Zhang, Y. W.; Fu, H.; Agama, K. K.; Tata, N.; Agrawal, S.; Aladjem, M. I.; Pommier, Y. Mus81-mediated DNA cleavage resolves replication forks stalled by topoisomerase I-DNA complexes. *J Cell Biol* **2011**, *195*, 739-749.
50. El-Khamisy, S. F.; Saifi, G. M.; Weinfeld, M.; Johansson, F.; Helleday, T.; Lupski, J. R.; Caldecott, K. W. Defective DNA single-strand break repair in spinocerebellar ataxia with axonal neuropathy-1. *Nature* **2005**, *434*, 108-113.

FIGURE LEGENDS

Figure 1: Compound 8 inhibits human Top1 catalytic activity both as recombinant enzyme and as an endogenous protein in the whole cell extracts of human breast adenocarcinoma (MCF7) cells. (A) Relaxation of supercoiled DNA with recombinant human Top1 at a molar ratio of 3:1. Lanes 1 and 9, pBS (SK⁺) DNA (90 fmol); lanes 2 and 10, same as lane 1, but incubated with 30 fmol of Top1; lanes 3 and 11, same as lane 2, but Top1 was incubated with 2% DMSO, lane 4, same as lane 2, but Top1 pre-incubated with 2 μ M CPT for 5 min; lanes 5-8, same as lane 2, but Top1 was pre-incubated with variable concentrations of compound **8** (as indicated) for 5 min followed by addition of DNA at 37°C for 15 min. Lane 12, same as lane 4, but CPT was incubated simultaneously with DNA and enzyme; lanes 13-16, same as lane 10, but simultaneously incubated with variable concentrations of compound **8** (as indicated) at 37°C for 15 min. **(B)** Schematic representation for preparation of MCF7 whole cell lysates which was used as the source of endogenous Top1 for *ex vivo* Top1 relaxation assays. **(C)** Relaxation of supercoiled pBS (SK⁺) DNA by Top1 activity from MCF7 cell extract (each reaction volume contains 0.1 μ g protein). Lanes 1 and 11, pBS (SK⁺) DNA (0.3 μ g); lane 2 and 3, same as lane 1, but DNA was incubated with MCF7 cell lysates; lanes 3 and 13, same as lane 2, but incubated with 2% DMSO, lanes 4 -10, same as lane 2, but MCF7 whole lysates were pre-incubated with 5 μ M CPT or the variable concentrations of compound **8** (as indicated) for 5 min followed by addition of DNA at 37°C for 15 min. lanes 14-20, same as lane 12, but MCF7 cell lysates were incubated simultaneously with 5 μ M of CPT or variable concentrations of compound **8** (as indicated) at 37°C for 15 min. Positions of supercoiled monomer (SM), relaxed and nicked monomer (RL/NM) are indicated. Quantitative representation for percentage relaxation inhibition (%) of recombinant Top1 **(D)** and endogenous Top1 **(E)** either pre-incubated or added

simultaneously with Top1 with the variable concentrations of compound **8**. All the experiments were performed three times and expressed as means \pm SD.

Figure 2: Compound 8 inhibits formation of Top1-DNA cleavage complexes and abrogates CPT-mediated DNA cleavage complex stabilization. (A) Representative gel showing Top1 mediated plasmid DNA cleavage in the presence of CPT or compound **8**. Lane 1, 50 fmol of pBS (SK⁺) supercoiled DNA. Lanes 2–9, same as lane 1 but incubated with equal amounts of recombinant human Top1 (100 fmol) at the indicated concentrations of CPT or compound **8** or only DMSO at 37°C for 30 min. Positions of supercoiled substrate (Form I) and nicked monomers (Form II) are indicated. **(B)** Experimental design to test the impact of compound **8** on CPT-mediated preformed Top1 cleavage complex (Top1cc). **(C)** Compound **8** abrogates CPT-mediated cleavage. Lane 1, 50 fmol of pBS (SK⁺) supercoiled DNA. Lanes 2-6, same as lane 1 but incubated with equal amounts of Top1 (100 fmol) at the indicated concentrations of CPT or compound **8**. Lanes 7-9, same as lane 1, but incubated with equal amounts of Top1 with CPT before addition of compound **8** as indicated at 37°C for 30 min. **(D)** Representative gel showing Top1-mediated 25 mer duplex oligonucleotide cleavage in the presence of CPT and compound **8**. Lane 1, 10 nM of 5'-³²P-end labeled 25 mer duplex oligo as indicated above. Lane 2, same as lane 1, but incubated with recombinant Top1 (0.2 μ M). Lanes 3-6, same as lane 2, but incubated with indicated concentration of CPT or compound **8**. Lanes 7-9, same as lane 2, but incubated with equal amounts of Top1 with CPT before addition of indicated concentrations of compound **8** at 37°C for 30 min. Positions of uncleaved oligonucleotide (25 mer) and the cleavage product (12 mer oligonucleotide complexed with residual Top1) are indicated. **(E)** Compound **8** inhibits formation of Top1-DNA bound complexes (Top1cc) in live cells. Representative images

showing the fluorescence recovery after photobleaching (FRAP) of enhanced green fluorescence tagged-human Top1 (EGFP-Top1) transiently expressed in MCF7 cells and their response to CPT (5 μ M), compound **8** (20 μ M) separately treated for 10 min or pretreatment with CPT (5 μ M) for 10 min followed by treatment of compound **8** (20 μ M) for 10 min (Pre CPT + **8**). A sub-nuclear spot (ROI) indicated by a circle was bleached (BLH) for 30 ms and photographed at regular intervals of 3 ms thereafter. Successive images taken for ~90 s after bleaching illustrate fluorescence return into the bleached areas. **(F)** Quantification of FRAP data (n=15) showing mean curves of Top1 in the presence of CPT or compound **8**. Error bars represent the standard error of the mean.

Figure 3: Compound 8 reversibly binds with Top1 at equimolar concentration. **(A)** Job's Plot of compound **8** binding to Top1. Data are represented as mean \pm SD from three independent experiments. **(B)** Double reciprocal plot of inhibitor binding to Top1. Data are represented as mean \pm SD from three independent experiments. **(C)** The linear plot of binding of compound **8** to Top1. Data are represented as mean \pm SD from three independent experiments. **(D)** Compound **8** binds with Top1 in reversible manner. Lane 1, 50 fmol of pBS (SK⁺) DNA. Lane 2, recombinant Top1 (100 fmol) was pre-incubated with the reaction mixture at 37⁰C for 5 min before addition of pBS (SK⁺) DNA. Lane 3, same as lane 2, but in presence of 2% v/v DMSO. Lane 4, same as lane 2, but in presence of 1 μ M of compound **8**, pre-incubated with Top1 for 5 min at 37⁰C in relaxation buffer followed by addition of 50 fmol of pBS (SK⁺) DNA and was further incubated for 15 min at 37⁰C. Lane 5–8, same as lane 4, but diluted to 5, 10, 20 and 40 fold so that the final inhibitor concentrations became 0.2, 0.1, 0.05 and 0.025 μ M of compound **8**. These were followed by addition of DNA and were further incubated for 15 min at 37⁰C. The experiments

were performed three times and representative result is from one set of experiments. **(E)** Compound **8**-DNA interaction as studied by agarose gel electrophoresis. Lane 1, 50 fmol of pBS (SK⁺) DNA. Lane 2, relaxed pBS (SK⁺) DNA generated by excess of Top1. Lanes 3–6, same as lane 2, but incubated with 50 and 300 μ M of m-AMSA and etoposide, respectively. Lanes 7–9, same as lane 2, but incubated with 50, 100, 300 μ M of compound **8** as indicated.

Figure 4: Compound 8 induces proteasome-mediated degradation of cellular Top1 and apoptotic PARP1 cleavage without stabilizing apoptotic Top1-DNA covalent complexes. (A)

Western blot analysis of Top1 in whole cell extracts of MCF7 cells treated with compound **8** (10 μ M) for indicated time. **(B)** Western blot analysis of Top1 in whole cell extracts from MCF7 cells without treatment (Lane 1) or treated with compound **8** (10 μ M) (Lane 2) or MG132 (100 nM; proteasome inhibitor) (Lane 3) or pre-incubated with MG132 for 4 h followed by addition of compound **8** for 12 h. Numbers are molecular masses in kilo Daltons. **(C)** Western blot analysis of PARP1 in whole cell extracts from MCF7 cells treated with compound **8** (10 μ M) for indicated times. Positions of PARP1 full length and cleaved PARP1 are indicated. **(D)** Detection of Top1cc by ICE bioassays in MCF7 cells treated with CPT (10 μ M) or compound **8** (20 μ M) for 12 h or pretreated with CPT for 6 h before the addition of compound **8** was further incubated for 6 h. Genomic DNA at increasing concentrations (0.5, 1, 2, 4 μ g) was probed with an anti-Top1 antibody. The bar represents quantification of Top1cc ($n = 3$; calculated value \pm S.E.M.) under different drug treatment. Asterisks denote significant difference (***) $P < 0.001$; t test).

Figure 5: Compound 8 activates reactive oxygen species (ROS)-induced oxidative DNA breaks and promotes apoptotic cell death. (A) Generation of ROS was measured using the

fluorescent dye CM-H2DCFDA in MCF7 cells after treatment with 0.2% DMSO alone (blue bar) or with 10 μ M compound **8** (red bar), and pre-treatment with N-acetylcysteine (NAC; 10 mM) for 30 min prior to treatment with compound **8** (yellow bar) for indicated times. Data are expressed as mean \pm S.D. of three independent experiments. **(B)** Representative images of alkaline comet assays with MCF7 cells treated with compound **8** for 12 h or pre-treatment with NAC (10 mM) for 30 min prior to treatment with compound **8** as indicated. **(C)** Quantification of drug induced mean comet tails were calculated for 20-25 cells (average \pm S.E.M). **(D)** Representative confocal microscopy images showing apoptosis marker phosphatidylserine as detected with Annexin V-FITC antibody (green) after compound **8** treatment for 12 h or pre-treatment with NAC (10 mM) for 30 min prior to compound **8** as indicated. Cells were counterstained with Propidium iodide (PI; red) to visualize nuclei. **(E)** Quantification of drug induced Annexin V (+) cells were calculated from \sim 100 cells (average \pm S.E.M) as indicated.

Figure 6: Compound 8 shows potent anticancer activity mediated through Topoisomerase

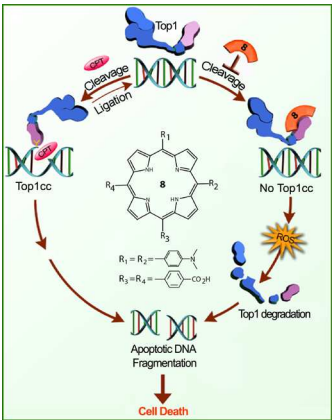
1. The graphical representation of percentage survival (%) of **(A)** MCF7, **(B)** HeLa, **(C)** HCT116, **(D)** NIH:OVCA-3, **(E)** HEK293, **(F)** MEFs (TDP+/+ and TDP-/-) cells was plotted as a function of indicated compound **8** concentrations. **(G)** Top1 knockdown cells are less sensitive to compound **8**. Following transfection with Top1 or control (Ctr) siRNA for 72 h, MCF7 cells were analyzed by Western blotting to confirm Top1 Knockdown. Actin served as loading control (inset). Percentage survival (%) of MCF7 cells transfected with Top1 or Ctr siRNA was plotted as a function of indicated compound **8** concentrations. **(H)** Graphical representation of percentage survival (%) of MCF7 cells treated with compound **8** or CPT separately or cells were pre-treatment with CPT (5 μ M) for 12 hr prior to addition of compound

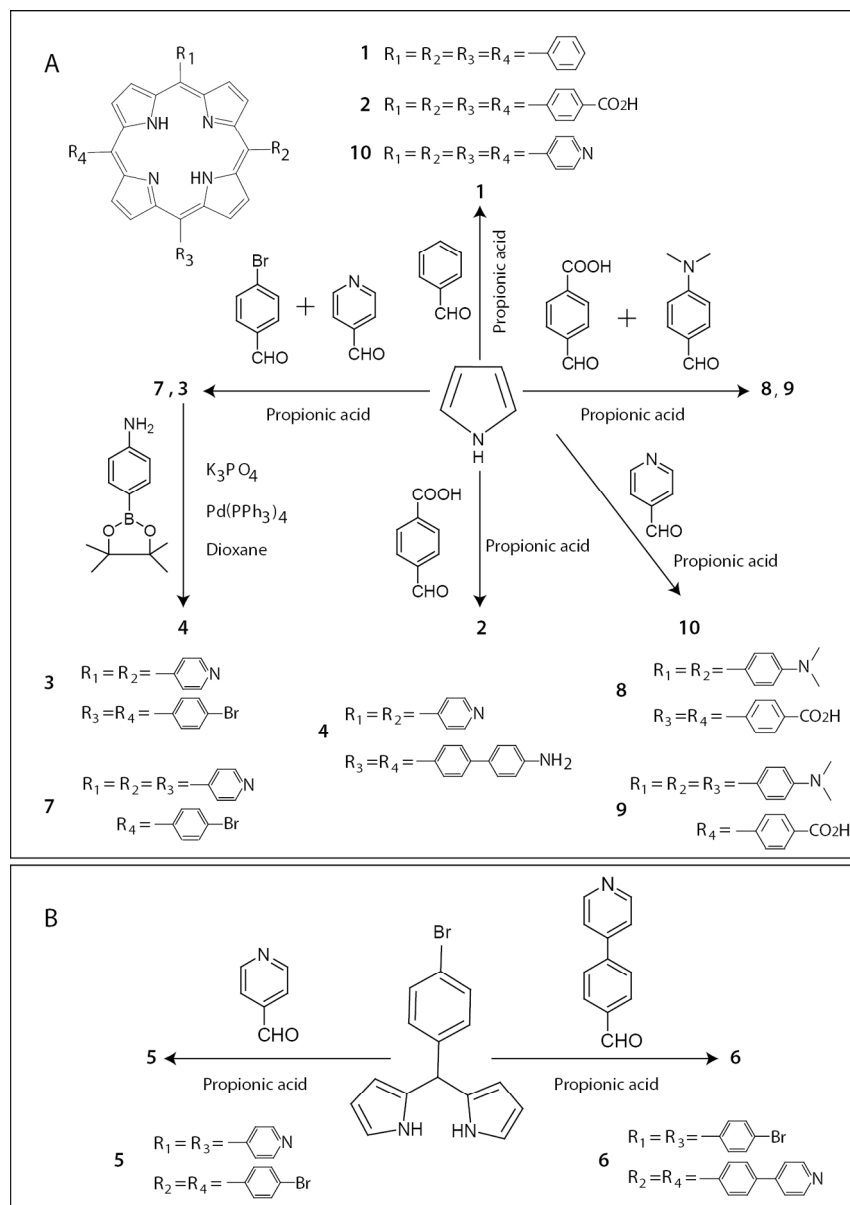
8 as indicated. The percent inhibition of viability for each concentration of compound **8** was calculated with respect to the control and IC_{50} (μM) values were estimated. Each point corresponds to the mean \pm S.D. of at least three experiments in duplicates. Error bars represent SD (n=3).

Scheme 1: Synthesis of library of Neutral porphyrin compounds.

Table 1. Effective drug concentrations (EC_{50}) of selected neutral porphyrin compounds on the recombinant human Top1 (Top1) plasmid DNA relaxation inhibition assays.

Table of Contents graphic.





Scheme 1: Synthesis of library of Neutral porphyrin compounds.

204x287mm (200 x 200 DPI)

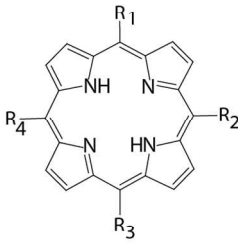
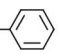
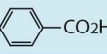



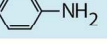

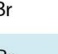
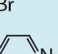

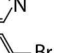
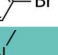


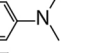
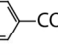
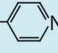
Core structure	Compound	Structure	Top1 inhibition EC ₅₀ (μM)	
			Simultaneous	Preincubation
	1	R ₁ = R ₂ = R ₃ = R ₄ = 	>50	>50
	2	R ₁ = R ₂ = R ₃ = R ₄ = 	2.015 ± 0.511	0.563 ± .19
	3	R ₁ = R ₂ =  R ₃ = R ₄ = 	>50	>50
	4	R ₁ = R ₂ =  R ₃ = R ₄ = 	82.78 ± 2.34	63.43 ± 1.89
	5	R ₁ = R ₃ =  R ₂ = R ₄ = 	>50	>50
	6	R ₁ = R ₃ =  R ₂ = R ₄ = 	>50	>50
	7	R ₁ = R ₂ = R ₃ =  R ₄ = 	>50	>50
	8	R ₁ = R ₂ =  R ₃ = R ₄ = 	1.472 ± .32	0.381 ± .11
	9	R ₁ = R ₂ = R ₃ =  R ₄ = 	1.972 ± 0.411	1.226 ± .14
	10	R ₁ = R ₂ = R ₃ = R ₄ = 	>50	>50

Table 1. Effective drug concentrations (EC50) of selected neutral porphyrin compounds on the recombinant human Top1 (Top1) plasmid DNA relaxation inhibition assays.

202x216mm (200 x 200 DPI)

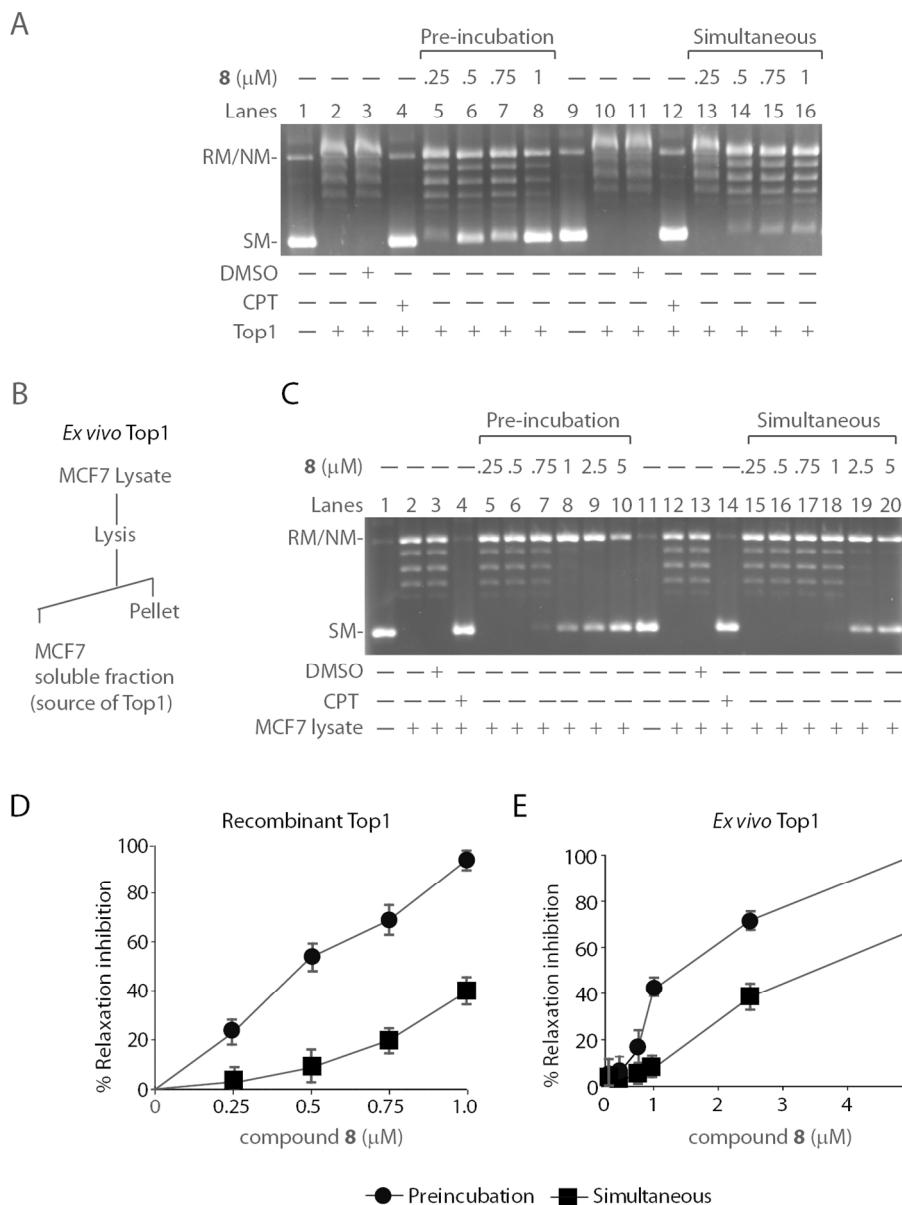


Figure 1: Compound 8 inhibits human Top1 catalytic activity both as recombinant enzyme and as an endogenous protein in the whole cell extracts of human breast adenocarcinoma (MCF7) cells. (A) Relaxation of supercoiled DNA with recombinant human Top1 at a molar ratio of 3:1. Lanes 1 and 9, pBS (SK+) DNA (90 fmol); lanes 2 and 10, same as lane 1, but incubated with 30 fmol of Top1; lanes 3 and 11, same as lane 2, but Top1 was incubated with 2% DMSO, lane 4, same as lane 2, but Top1 pre-incubated with 2 μM CPT for 5 min; lanes 5-8, same as lane 2, but Top1 was pre-incubated with variable concentrations of compound 8 (as indicated) for 5 min followed by addition of DNA at 37°C for 15 min. Lane 12, same as lane 4, but CPT was incubated simultaneously with DNA and enzyme; lanes 13-16, same as lane 10, but simultaneously incubated with variable concentrations of compound 8 (as indicated) at 37°C for 15 min. (B) Schematic representation for preparation of MCF7 whole cell lysates which was used as the source of endogenous Top1 for ex vivo Top1 relaxation assays. (C) Relaxation of supercoiled pBS (SK+) DNA by Top1 activity from MCF7 cell extract (each reaction volume contains 0.1 μg protein). Lanes 1 and 11, pBS (SK+) DNA (0.3 μg); lane 2 and 3, same as lane 1, but DNA was incubated with MCF7 cell lysates; lanes 3 and 13,

same as lane 2, but incubated with 2% DMSO, lanes 4 -10, same as lane 2, but MCF7 whole lysates were pre-incubated with 5 μ M CPT or the variable concentrations of compound 8 (as indicated) for 5 min followed by addition of DNA at 37°C for 15 min. lanes 14-20, same as lane 12, but MCF7 cell lysates were incubated simultaneously with 5 μ M of CPT or variable concentrations of compound 8 (as indicated) at 37°C for 15 min. Positions of supercoiled monomer (SM), relaxed and nicked monomer (RL/NM) are indicated. Quantitative representation for percentage relaxation inhibition (%) of recombinant Top1 (D) and endogenous Top1 (E) either pre-incubated or added simultaneously with Top1 with the variable concentrations of compound 8. All the experiments were performed three times and expressed as means \pm SD.

178x234mm (200 x 200 DPI)

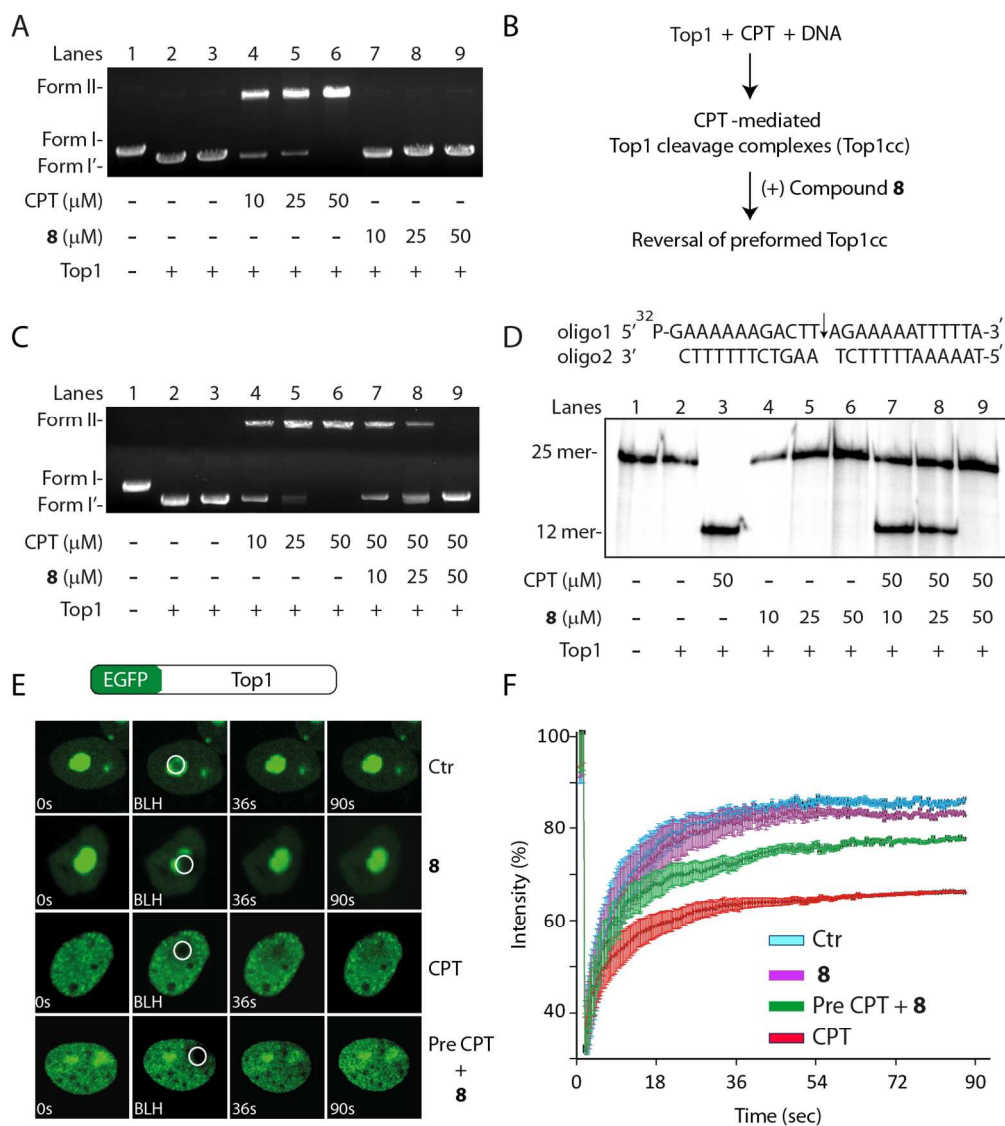


Figure 2: Compound **8** inhibits formation of Top1-DNA cleavage complexes and abrogates CPT-mediated DNA cleavage complex stabilization. (A) Representative gel showing Top1 mediated plasmid DNA cleavage in the presence of CPT or compound **8**. Lane 1, 50 fmol of pBS (SK+) supercoiled DNA. Lanes 2–9, same as lane 1 but incubated with equal amounts of recombinant human Top1 (100 fmol) at the indicated concentrations of CPT or compound **8** or only DMSO at 37°C for 30 min. Positions of supercoiled substrate (Form I) and nicked monomers (Form II) are indicated. (B) Experimental design to test the impact of compound **8** on CPT-mediated preformed Top1 cleavage complex (Top1cc). (C) Compound **8** abrogates CPT-mediated cleavage. Lane 1, 50 fmol of pBS (SK+) supercoiled DNA. Lanes 2–6, same as lane 1 but incubated with equal amounts of Top1 (100 fmol) at the indicated concentrations of CPT or compound **8**. Lanes 7–9, same as lane 1, but incubated with equal amounts of Top1 with CPT before addition of compound **8** as indicated at 37°C for 30 min. (D) Representative gel showing Top1-mediated 25 mer duplex oligonucleotide cleavage in the presence of CPT and compound **8**. Lane 1, 10 nM of 5'-³²P-end labeled 25 mer duplex oligo as indicated above. Lane 2, same as lane 1, but incubated with recombinant Top1 (0.2 μ M). Lanes 3–6, same as lane 2, but incubated with indicated concentration of CPT or compound **8**. Lanes 7–9, same as lane 2, but incubated with equal amounts of Top1 with CPT before addition of indicated concentrations of compound **8** at 37°C for 30 min. Positions of uncleaved oligonucleotide (25 mer) and the cleavage product

(12 mer oligonucleotide complexed with residual Top1) are indicated. (E) Compound 8 inhibits formation of Top1-DNA bound complexes (Top1cc) in live cells. Representative images showing the fluorescence recovery after photobleaching (FRAP) of enhanced green fluorescence tagged-human Top1 (EGFP-Top1) transiently expressed in MCF7 cells and their response to CPT (5 μ M), compound 8 (20 μ M) separately treated for 10 min or pretreatment with CPT (5 μ M) for 10 min followed by treatment of compound 8 (20 μ M) for 10 min (Pre CPT + 8). A sub-nuclear spot (ROI) indicated by a circle was bleached (BLH) for 30 ms and photographed at regular intervals of 3 ms thereafter. Successive images taken for ~90 s after bleaching illustrate fluorescence return into the bleached areas. (F) Quantification of FRAP data (n=15) showing mean curves of Top1 in the presence of CPT or compound 8. Error bars represent the standard error of the mean.

203x226mm (200 x 200 DPI)

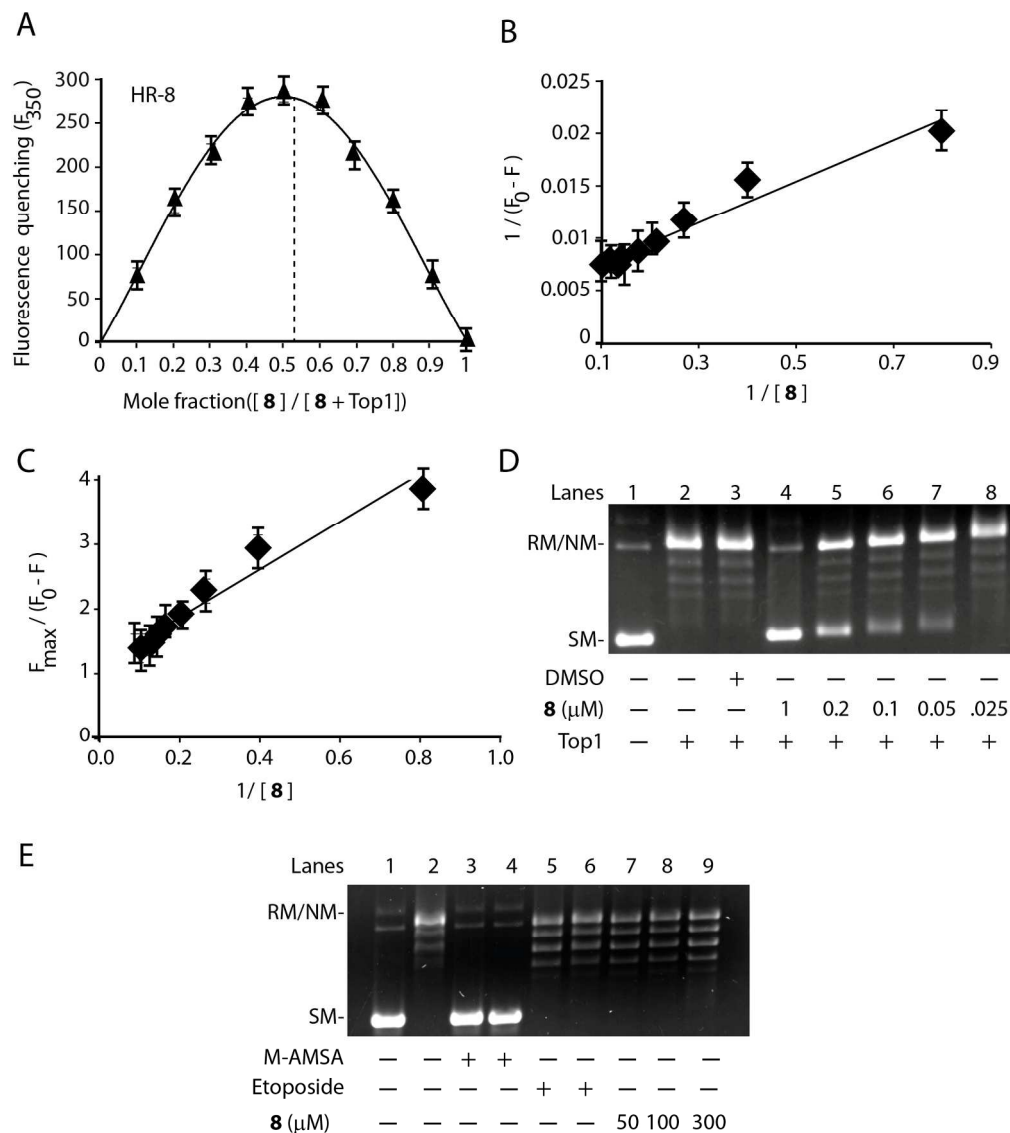


Figure 3: Compound 8 reversibly binds with Top1 at equimolar concentration. (A) Job's Plot of compound 8 binding to Top1. Data are represented as mean \pm SD from three independent experiments. (B) Double reciprocal plot of inhibitor binding to Top1. Data are represented as mean \pm SD from three independent experiments. (C) The linear plot of binding of compound 8 to Top1. Data are represented as mean \pm SD from three independent experiments. (D) Compound 8 binds with Top1 in reversible manner. Lane 1, 50 fmol of pBS (SK+) DNA. Lane 2, recombinant Top1 (100 fmol) was pre-incubated with the reaction mixture at 370C for 5 min before addition of pBS (SK+) DNA. Lane 3, same as lane 2, but in presence of 2% v/v DMSO. Lane 4, same as lane 2, but in presence of 1 μM of compound 8, pre-incubated with Top1 for 5 min at 370C in relaxation buffer followed by addition of 50 fmol of pBS (SK+) DNA and was further incubated for 15 min at 370C. Lane 5–8, same as lane 4, but diluted to 5, 10, 20 and 40 fold so that the final inhibitor concentrations became 0.2, 0.1, 0.05 and 0.025 μM of compound 8. These were followed by addition of DNA and were further incubated for 15 min at 370C. The experiments were performed three times and representative result is from one set of experiments. (E) Compound 8-DNA interaction as studied by agarose gel electrophoresis. Lane 1, 50 fmol of pBS (SK+) DNA. Lane 2, relaxed pBS (SK+) DNA generated by excess of Top1. Lanes 3–6, same as lane 2, but incubated with 50 and 300 μM of m-AMSA and etoposide, respectively. Lanes 7–9, same as lane 2, but incubated with 50, 100, 300 μM of compound 8 as indicated.

1
2
3
4
5
6
7
8
9
10
11
12
13
14
15
16
17
18
19
20
21
22
23
24
25
26
27
28
29
30
31
32
33
34
35
36
37
38
39
40
41
42
43
44
45
46
47
48
49
50
51
52
53
54
55
56
57
58
59
60

190x216mm (300 x 300 DPI)

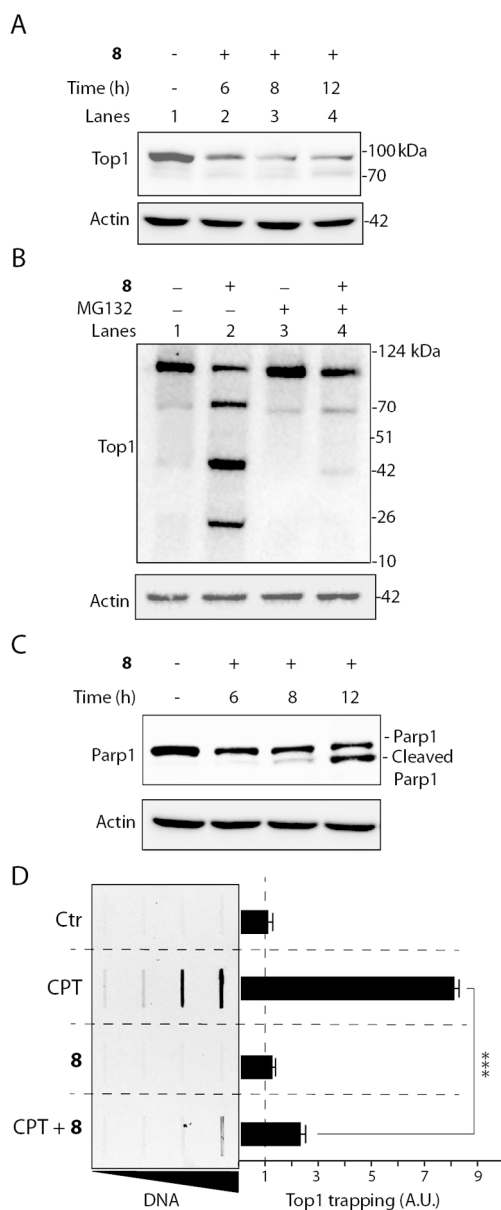


Figure 4: Compound 8 induces proteasome-mediated degradation of cellular Top1 and apoptotic PARP1 cleavage without stabilizing apoptotic Top1-DNA covalent complexes. (A) Western blot analysis of Top1 in whole cell extracts of MCF7 cells treated with compound 8 (10 μ M) for indicated time. (B) Western blot analysis of Top1 in whole cell extracts from MCF7 cells without treatment (Lane 1) or treated with compound 8 (10 μ M) (Lane 2) or MG132 (100 nM; proteasome inhibitor) (Lane 3) or pre-incubated with MG132 for 4 h followed by addition of compound 8 for 12 h. Numbers are molecular masses in kilo Daltons. (C) Western blot analysis of PARP1 in whole cell extracts from MCF7 cells treated with compound 8 (10 μ M) for indicated times. Positions of PARP1 full length and cleaved PARP1 are indicated. (D) Detection of Top1cc by ICE bioassays in MCF7 cells treated with CPT (10 μ M) or compound 8 (20 μ M) for 12 h or pretreated with CPT for 6 h before the addition of compound 8 was further incubated for 6 h. Genomic DNA at increasing concentrations (0.5, 1, 2, 4 μ g) was probed with an anti-Top1 antibody. The bar represents quantification of Top1cc ($n = 3$; calculated value \pm S.E.M.) under different drug treatment. Asterisks denote significant difference (***) $P < 0.001$; t test).

1
2
3
4
5
6
7
8
9
10
11
12
13
14
15
16
17
18
19
20
21
22
23
24
25
26
27
28
29
30
31
32
33
34
35
36
37
38
39
40
41
42
43
44
45
46
47
48
49
50
51
52
53
54
55
56
57
58
59
60

112x272mm (200 x 200 DPI)

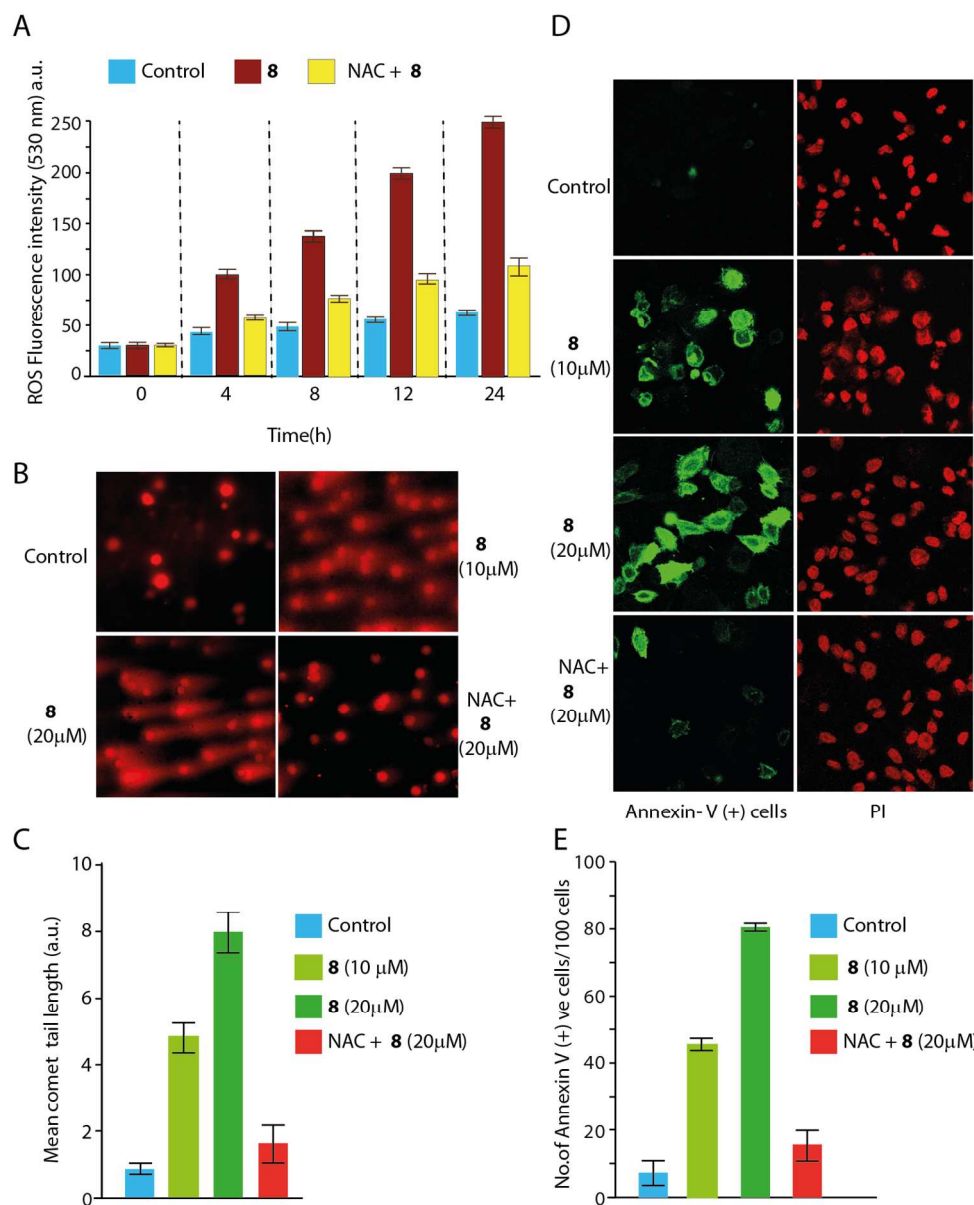


Figure 5: Compound 8 activates reactive oxygen species (ROS) oxidative DNA breaks and promotes apoptotic cell death. (A) Generation of ROS was measured using the fluorescent dye CM-H2DCFDA in MCF7 cells after treatment with 0.2% DMSO alone (blue bar) or with 10 μM compound 8 (red bar), and pre-treatment with N-acetylcysteine (NAC; 10 mM) for 30 min prior to treatment with compound 8 (yellow bar) for indicated times. Data are expressed as mean ± S.D. of three independent experiments. (B) Representative images of alkaline comet assays with MCF7 cells treated with compound 8 for 12 h or pre-treatment with NAC (10 mM) for 30 min prior to treatment with compound 8 as indicated. (C) Quantification of drug induced mean comet tails were calculated for 20-25 cells (average ± S.E.M). (D) Representative confocal microscopy images showing apoptosis marker phosphatidylserine as detected with Annexin V-FITC antibody (green) after compound 8 treatment for 12 h or pre-treatment with NAC (10 mM) for 30 min prior to compound 8 as indicated. Cells were counterstained with Propidium iodide (PI; red) to visualize nuclei. (E) Quantification of drug induced Annexin V (+) cells were calculated from ~100 cells (average ± S.E.M) as indicated.

1
2
3
4
5
6
7
8
9
10
11
12
13
14
15
16
17
18
19
20
21
22
23
24
25
26
27
28
29
30
31
32
33
34
35
36
37
38
39
40
41
42
43
44
45
46
47
48
49
50
51
52
53
54
55
56
57
58
59
60

203x248mm (200 x 200 DPI)

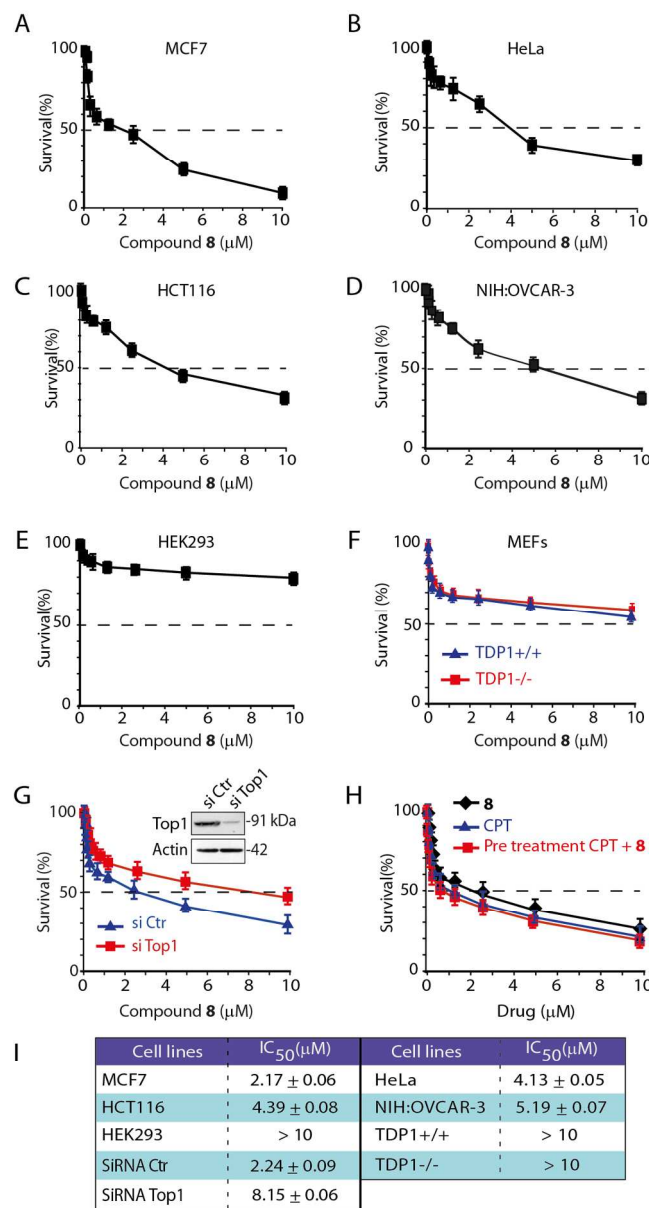


Figure 6: Compound 8 shows potent anticancer activity mediated through Topoisomerase 1. The graphical representation of percentage survival (%) of (A) MCF7, (B) HeLa, (C) HCT116, (D) NIH:OVCA-3, (E) HEK293, (F) MEFs (TDP+/+ and TDP-/-) cells was plotted as a function of indicated compound 8 concentrations. (G) Top1 knockdown cells are less sensitive to compound 8. Following transfection with Top1 or control (Ctr) siRNA for 72 h, MCF7 cells were analyzed by Western blotting to confirm Top1 Knockdown. Actin served as loading control (inset). Percentage survival (%) of MCF7 cells transfected with Top1 or Ctr siRNA was plotted as a function of indicated compound 8 concentrations. (H) Graphical representation of percentage survival (%) of MCF7 cells treated with compound 8 or CPT separately or cells were pre-treatment with CPT (5 μM) for 12 hr prior to addition of compound 8 as indicated. The percent inhibition of viability for each concentration of compound 8 was calculated with respect to the control and IC_{50} (μM) values were estimated. Each point corresponds to the mean \pm S.D. of at least three experiments in duplicates. Error bars represent SD ($n=3$).

1
2
3
4
5
6
7
8
9
10
11
12
13
14
15
16
17
18
19
20
21
22
23
24
25
26
27
28
29
30
31
32
33
34
35
36
37
38
39
40
41
42
43
44
45
46
47
48
49
50
51
52
53
54
55
56
57
58
59
60

154x291mm (200 x 200 DPI)